AD-A129 350 THE COOLING OF PRINTED CIRCUIT BOARD MOUNTED COMPONENTS 1/1
USING COPPER LADD..(U) ROYAL AIRCRAFT ESTABLISHMENT
FARNBOROUGH (ENGLAND) I C DALE SEP 82 RAE-TR-82092
UNCLASSIFIED DRIC-BR-86157 F/G 1/3 NL

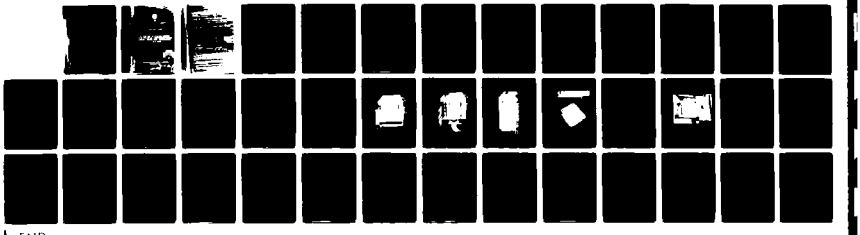

END
DATE FILMED
DTIC

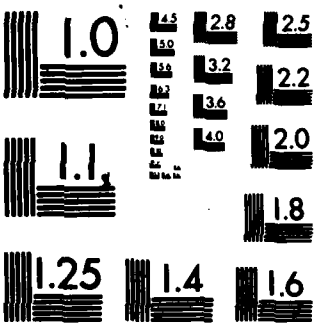

MICROCOPY RESOLUTION TEST CHART
NATIONAL BUREAU OF STANDARDS-1963-A

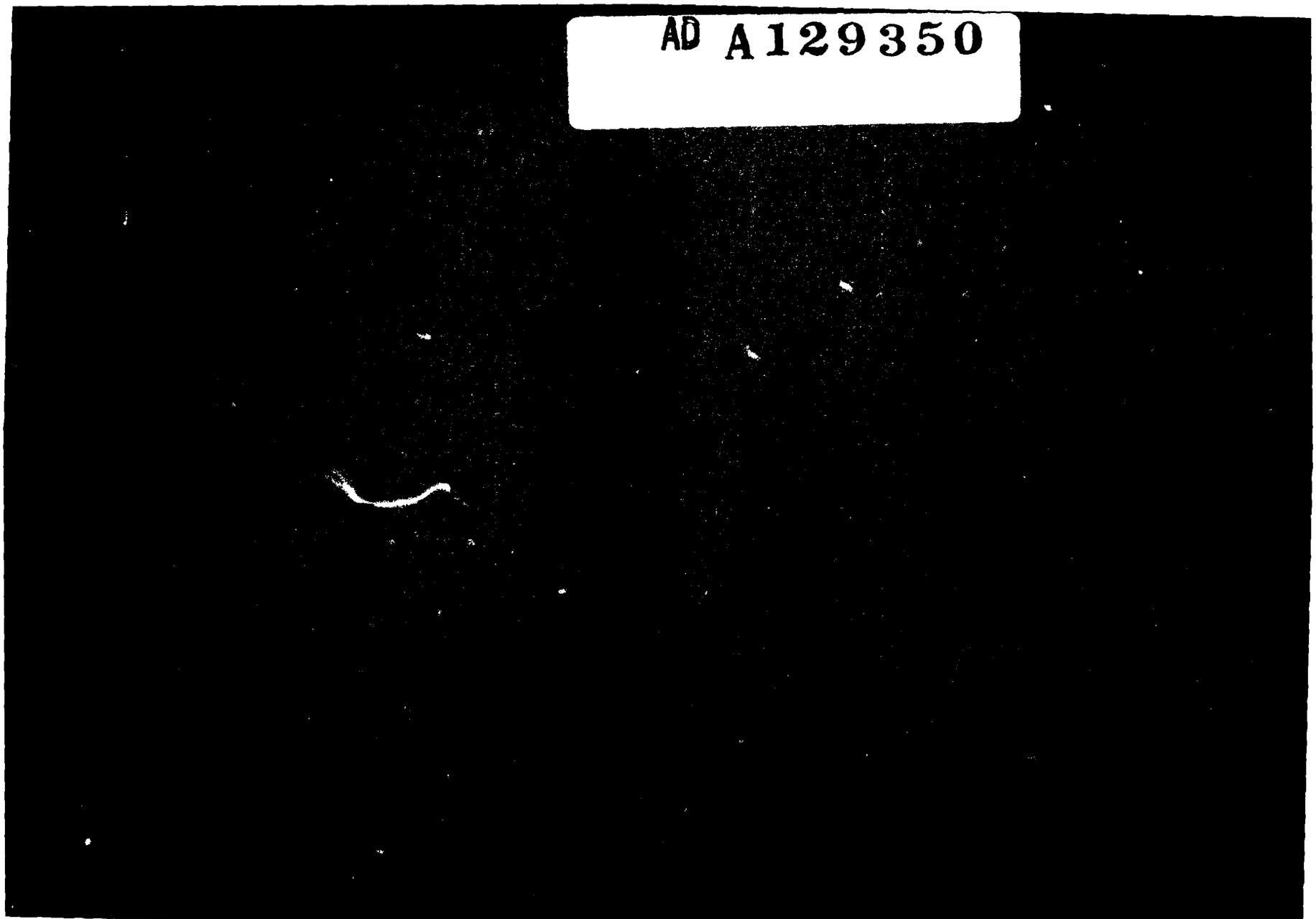

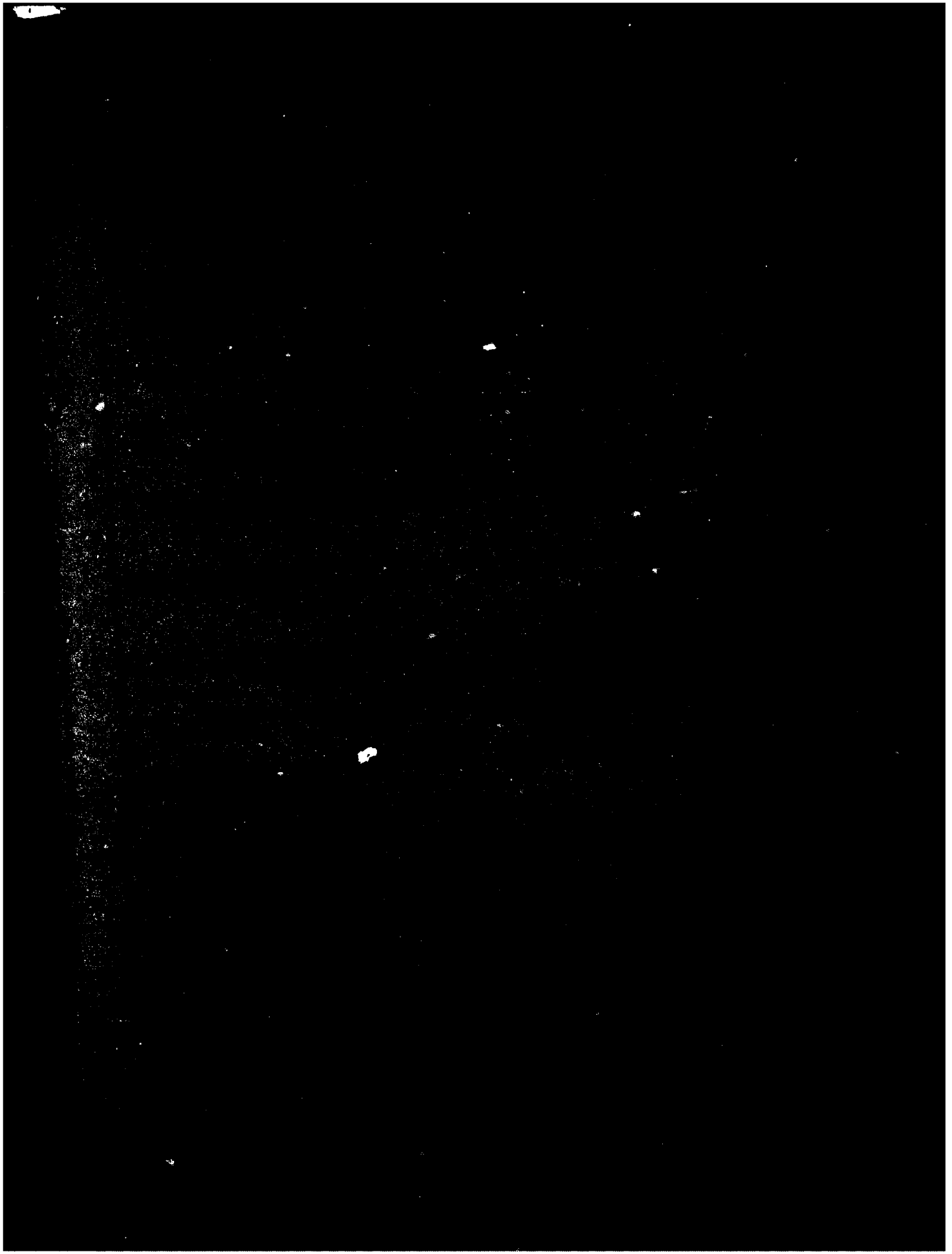

UDC 621.38-71 : 621.3.049.75

ROYAL AIRCRAFT ESTABLISHMENT

Technical Report 82092

Received for printing 1 September 1982

THE COOLING OF PRINTED CIRCUIT BOARD MOUNTED COMPONENTS USING COPPER LADDER HEAT CONDUCTION TO A COLD WALL

by

I. C. Dale

SUMMARY

This Report describes a series of experimental tests, designed to investigate the cooling of printed circuit board (PCB) mounted dual-in-line (DIL) components within an avionic box using the copper ladder/cold wall technique. Areas of investigation include avionic box orientation, side wall conduction, top plate finning, mixed 'air-wash', avionic power reduction, cooling air temperature reduction, cooling air mass flowrate reduction, cold wall heat pick-up and avionic box insulation.

Results were obtained from thermocouple temperature measurements, details of the instrumentation used as well as the thermocouple and component layout within the avionic box are included.

The use of an aluminium alloy 'interplate' to cool two adjacent PCBs is also discussed.

Results in graphical form are included together with a list of conclusions on the effects of all the major parameters considered.

Departmental Reference: FS(F) 184

LIST OF CONTENTS

		Page
1	INTRODUCTION	3
2	RANGE OF INVESTIGATION	3
3	DESCRIPTION OF TEST EQUIPMENT	4
4	PROCEDURE	6
5	RESULTS AND DISCUSSION	7
6	CONCLUSIONS	11
Table 1	Summary of test results	13
References		15
Illustrations		Figures 1-23
Report documentation page		inside back cover

1 INTRODUCTION

In current fighter aircraft, the avionics may form 70-80% of the total Environmental Control System (ECS) cooling load[1] and the continual demand for yet more avionic equipment emphasises the importance of future avionic cooling design. Zara *et al*[2] have stated that "avionic systems have required more maintenance than any other system, and, due to their complexity, utilize more than 50% of the total logistic support dollars for fighter and bomber weapon systems".

Cost and reliability benefits may be achieved by reducing the operating temperature of many components, using good heat transfer design within avionic equipment.

Previously, heat removal was often accomplished by simply blowing cool air through the boxes concerned. Experience has shown that this 'air-wash' method of cooling has certain disadvantages such as shielding, whereby some components may be starved of cooling air due to their size, shape or position. Thus structural design and internal layout needs to be considered if overheating is to be avoided. Furthermore, if cockpit exhaust air is used as the coolant, there is a risk of introducing contaminants (oil, sweat etc) into the box which could lead to corrosion and eventual failure.

An alternative method of cooling, avoiding some of the disadvantages of the air-wash system, is to use a 'cold wall' which is basically a heat exchanger, forming an integral part of the equipment, through which coolant is passed. The design of the equipment is such that heat conduction paths are provided from power dissipating components to the cold wall. For example, where dual-in-line (DIL) components are used on printed circuit boards (PCBs) use is made of copper strip (*ie* a copper ladder) to conduct the heat to the cold wall. To optimise design there is a need to understand the heat transfer processes and recognise the importance of other heat transfer paths, and if necessary exploit them. For this purpose a simulated cold wall avionic 'black box' was constructed, incorporating a known heat load distribution and fitted with copper ladder cooled PCBs. The avionic box was operated under various ambient conditions, and by means of extensive instrumentation the influence of certain design changes on component temperatures was observed.

2 RANGE OF INVESTIGATION

Tests were performed on a simulated black box which was extensively instrumented for the purpose of thermal studies. The box represented a conventional copper ladder/ cold wall design.

Previous work[3] had shown that with equipment of a given geometry it is advantageous if a cold wall is provided at each end of the PCBs, component temperatures being substantially reduced by this method of cooling. With cold plank cooling, where the heat sink, equivalent to the cold wall, is a part of the aircraft structure on which the equipment is mounted, it is not practicable to provide other than a single heat sink. Furthermore the use of cold plank cooling means that a heat sink is likely to be at the bottom of the equipment. If, however there is a low thermal

resistance path between the top of the avionic box casing and the bottom (*ie* the cold wall or cold plank) then the top of the box would itself behave to some extent like a cold wall.

The tests were therefore designed to investigate, among other things, the part played by the side walls of the equipment in transferring heat from the top of the avionic box to the cold wall, and also to determine whether the provision of heat pipes would in any way help the process.

In some aircraft, the equipment bay may never reach a particularly high temperature and bay ambient air may be a useful heat sink during much of the flight. Under these circumstances it would appear advantageous to enhance the heat loss from the top of the equipment by means of suitable finning, and hence this was also investigated.

A limited number of tests were made with the equipment totally insulated from the ambient surroundings, *ie* heat loss was via the cold wall only.

Also investigated was an arrangement whereby, instead of using copper ladders for heat conduction to the cold wall, an aluminium alloy plate was positioned between two adjacent PCBs and served as a common heat path to the cold wall.

A limited number of tests were made to establish the effect on component temperatures of providing air-wash cooling in addition to the existing conduction arrangements. The effects on component temperature of equipment orientation, power variation, cold wall air mass flowrate and inlet temperature were also investigated.

3 DESCRIPTION OF TEST EQUIPMENT

The dimensions of the simulated avionic box (353 mm × 188 mm × 194 mm) used for these tests (Fig 1) differed only slightly from the standard 3/4 ATR short box. The base of the avionic box housed a cold wall heat exchanger (Fig 2) the inner surface of the base being machined to provide the lower guides for the PCBs. The heat exchanger, which consisted of a single layer of corrogation, measured 182 mm wide × 6.35 mm deep with 630 aluminium alloy fins per metre, the fin thickness being 0.15 mm. The heat exchanger inlet and outlet consisted of connector block assemblies as shown in Fig 3. All surfaces of the aluminium alloy box were anodised black, however the outer surface of the base was made from plain aluminium alloy sheet. The inner surface of the roof was machined to provide the upper guides for the PCBs. The 2.5mm thick front and rear walls of the box were fitted with carrying handles, together with inlet ducts used for experiments involving air-wash cooling. The 3.1mm thick side walls were machined to fit around their respective connector block assembly, the front edge of one side wall being suitably cut to allow sheathed thermocouple wires to be led out of the box (Fig 4).

Four copper heat pipes (ISOTERIX TYPE TX 2002C) were incorporated into the avionic box. Positioned vertically, they connected the roof via corner blocks at the upper surface of the box, to the inlet and outlet connector blocks of the cold wall. The 6.35mm diameter heat pipes were securely clamped into position leaving 25 mm of the 200mm long pipes protruding through the roof.

A total of 15 PCBs were installed inside the avionic box; on each board were mounted 35 DIL integrated circuits which were electrically in parallel and connected through their power supply pins only. The 14 pin DILs were positioned in contact with the copper ladders using a set layout of seven columns by five rows, per PCB. The ladders were attached to the PCBs using two small screws and a thin film of epoxy adhesive. An easy-break proprietary adhesive cement was used to attach the DILs to the copper ladders. The latter simplified the task of soldering the pins to the PCB whilst promoting good heat transfer from the DILs to the ladder[3]. As shown in Fig 5, the 0.914mm thick nickel plated copper ladders had a total of seven 'rungs' (4 mm wide) the ends of each 'rung' leading into an end strip (6 mm wide), which was held in contact with the guides by a berylium copper leaf spring (0.34 mm thick) screwed on to the horizontal edges of the PCB on the printed circuit side of the board.

Only 13 of the 15 PCBs were fitted with copper ladders, the two remaining PCBs relying on an aluminium alloy 'interplate' for heat conduction to the cold wall (Fig 1). The interplate, like the copper ladders, connected the roof with the cold wall, the ends of the interplate being held centrally within the raised sections of the PCB guides. The two PCBs either side of the interplate (having the same component layout pattern as boards fitted with ladders) were positioned to allow the upper surface of the DILs to make contact with the interplate once the PCBs were lightly screwed together. These two PCBs measured 158 mm × 150 mm and 138 mm × 150 mm compared with 177 mm × 150 mm for the remainder, fitted with copper ladders.

The power supply unit was positioned at the cooling air outlet end of the avionic box and occupied approximately 20% of the total internal volume. The unit was mainly constructed from a logic system stabilised power supply (Type LC REG 5V5A) manufactured by Weir Instrumentation Limited. Power consumption for this unit remained almost constant at 30-32 W. This unit was used only to provide an appropriate heat load and not to power the PCBs, the latter being supplied by three Coutant dc power supply units, external to the avionic box.

Two thin mica sheets were positioned within the avionic box, each sheet being held midway between two adjacent PCBs. Attached to the vertical centre line of the mica sheets were a total of seven copper-constantan thermocouples, which where used to measure internal ambient temperatures.

Fig 6 shows the layout of PCBs inside the avionic box, which remained the same for all tests. Installed within the box were a total of 85 fine gauge (0.15 mm) copper-constantan thermocouples, of which 53 were bonded to individual DILs (*ie* the DIL case), and a further 25 were attached to various parts of the box. The remaining seven thermocouples were those attached to thin mica sheets as described above.

A Solartron data logger (Series II) was used to record the thermocouple readings; output was obtained in both paper tape and typewriter print-out form.

Cooling air temperatures were measured by thermocouples inserted into each leg of the bifurcated (Y tube) inlet and outlet ducts. The four thermocouples were monitored using a digital voltmeter via a selection box.

There were two separately powered PCB circuits. The power consumption of each group of PCBs was obtained by measuring the appropriate voltages and currents, the latter in terms of a voltage drop over a standard resistance connected in series. Knowing the power taken by the power supply unit (measured using a wattmeter) the total avionic power was calculated.

A small electrical air blower provided the necessary flow of cooling air, which was measured using a 'Rotameter' flowmeter. A single thermocouple, positioned just downstream of the flowmeter and coupled to a portable potentiometer, provided accurate air temperature readings from which the true mass flowrate was calculated. Prior to entry into the avionic box, the cooling air passed through a tube wound with an electrical heater tape, thus the cooling air could be maintained at a selected temperature.

The avionic box was positioned centrally within a purpose built insulated wooden chamber, which enabled elevated bay temperatures to be simulated. Temperature control was automatic, (with pre-set facility) heat being provided by two rows of heater bars attached to the vertical sides of the chamber. Fig 7 shows the layout within the chamber, including the electric fan which circulated bay (ambient) air during tests. Fig 7 also shows the sheathed thermocouple wires together with the power supply cables terminating at the connector fitted to the rear of the avionic box. The box was placed on top of a thick polystyrene slab for all tests except those which investigated the effect of ambient air circulation beneath the cold wall when the box was mounted on Tufnol blocks.

During assembly of the avionic box, great care was taken to ensure good thermal contact between the various components, *ie* air gaps were avoided where possible, screws were fully tightened and thermal grease was used wherever necessary.

4 PROCEDURE

Having decided the layout within the avionic box, (PCB positions, etc) the box was placed within the wooden chamber, the power supply cables were connected and the chamber lid was placed firmly into position. Glass thermometers, inserted through the lid and positioned at various levels within the chamber were used to determine bay temperature, and to check for stratification. A sheathed thermistor was included as part of the bay air control instrumentation. With the cooling air supply turned on, the flowrate was adjusted by bleeding excess cooling air direct to atmosphere. The instrumentation used to control the bay and cooling air temperatures was then switched on, the respective controls being pre-set according to requirements.

The data logger, output typewriter and tape punch were then switched on and the scan command interval adjusted as required. An initial scan showed if any thermocouples were not functioning correctly.

With the power supply unit (fitted within the avionic box) and the dc voltage supplies to the PCBs switched on, DIL temperatures were monitored automatically at regular intervals to check thermal stability. This was judged to have been reached when three successive scans gave the same readings. A further scan was then taken and recorded. Cooling air flowrate, chamber bay air temperature and avionic supply power consumption readings were noted as were the cooling air inlet and outlet temperatures.

Each test configuration was operated at several bay temperatures (usually four) taking care not to exceed the manufacturer's stated maximum operating temperature for the components.

The paper tape outputs were used as input for an ALGOL computer program. Some of the program output results are included in graphical form in this Report.

5 RESULTS AND DISCUSSION

The results of the experimental investigation are summarised in Table 1. A total of 14 tests were completed each covering a range of bay temperatures spanning approximately 20-70°C. In Run 1, considered to be the standard (baseline) test, the total power (*ie* PCBs plus power supply unit) was set at 138 W with a cold wall airflow nominally set at the recommended ARINC 404A flowrate of 21.8 kg h^{-1} 100 W^{-1}. The average DIL temperature (*ie* the mean measured temperature of the instrumented DILs mounted on copper ladders) varied almost linearly with bay temperature. As shown in Fig 8, a change in bay temperature from 40-70°C caused an 11°C rise in average DIL temperature indicating that the effect of bay temperature on component temperature is ameliorated by cold wall cooling as expected.

Calculation of the heat radiated from the top of the avionic box showed that the heat loss was small, varying from 14 W to 4 W over the ambient temperature range 23-70°C. Convective cooling from the top surface was also small, typically 8 W at 23°C ambient temperature (based on the measured air velocity within the chamber).

For Run 2, the avionic box was inverted such that the cold wall was uppermost. In this configuration the four heat pipes were oriented for optimum heat transfer from the roof to the cold wall, the condenser end of each pipe being above the evaporator. In this position the four heat pipes could each transfer approximately 200 W, thereby creating in effect, a second cold wall.

Test results however (Fig 8) show that DIL temperatures were not reduced with the box inverted, indeed average DIL temperatures increased approximately 2°C over the entire bay temperature range. This was partly due to the increased heat flowrate to the cold wall, caused by the exposure of the outer surface of the cold wall to the bay (ambient) air.

Heat losses from the top of the box are known to be small (see above), and cooling by radiation and natural convection of the copper ladder mounted components within the box is minimal[3]. It may be concluded that because component temperatures altered only slightly when the box was inverted, the heat pipes were contributing very little to the cooling performance. This point is further emphasised by the fact that the top plate temperatures were very similar for the normal and inverted box positions.

It is suggested that a high thermal resistance at the heat pipe clamps which were difficult to align correctly, may account for the inadequate performance of the pipes. Subsequent tests were all performed with the simulated avionic box restored to its normal upright position.

Run 3, in which the metal sides of the box were replaced with insulating (bakelite) material, produced almost identical DIL temperatures (Fig 8) to those in Run 1. This implies that heat flow down the metal sides of the avionic box was very small, having little influence on component temperatures.

For Run 4, finning was provided on the top of the avionic box to enhance heat loss to the bay. Good thermal contact was ensured by the application of thermal grease between the finned plate and the box. Both the box and the radiating surfaces of the plate were anodised black. Results show that average DIL temperatures (compared with Run 1) were reduced by only $1\frac{1}{2}$-3°C (Fig 8) over the series of simulated bay temperatures. It is noteworthy that the increased heat loss to the bay was accompanied by a reduced heat flowrate to the cold wall (Table 1).

Run 5 was intended to give an indication of the effectiveness of air-wash, *ie* the provision of an air supply to the interior of the box to directly cool the components. For convenience, the cold wall exit air was used for this purpose, thus components were cooled both by heat conduction to the cold wall and air-wash (mixed air-wash) in this case. Run 6 was a repeat of Run 5 at a lower total power level. The results of these tests are compared with corresponding cold wall cooling only tests (*ie* Runs 1 and 7) in Fig 9. It can be seen that at full power (138 W) the addition of air-wash reduced component temperatures by about 11°C over the range of ambient temperatures. The corresponding tests at reduced avionic power (Runs 6 and 7) showed that air-wash lowered component temperatures by approximately 6.5°C. Air-wash is therefore clearly beneficial; the attendant disadvantages have been noted in section 1.

Fig 9 also shows how average DIL temperature was influenced by avionic power consumption. The total power dissipation, normally maintained at approximately 138 W, included the power supply unit plus the power taken by the PCBs. This was reduced in Runs 6 and 7 to 111 W (80% of 138 W) by lowering the voltage across the PCBs, the power taken by the power supply unit being fixed. Similarly the cooling air mass flowrate was reduced in proportion from 8.21×10^{-3} kg/s to 6.65×10^{-3} kg/s (approximately). As shown in Fig 9, the net result of reducing the power consumption in a standard (conduction cooled) box was to reduce DIL temperatures by between 8.5° and 6.5°, over the entire bay ambient temperature range. The same power reduction in the combined air-wash/cold wall cooled arrangement reduced component temperatures by between 4° and 2°. As indicated above and shown in Fig 9, the combined effects of air-wash cooling plus avionic power reduction (compare Runs 1 and 6) reduced average DIL temperatures between 15-13°.

Fig 10 shows the effect inlet temperature reduction has an average DIL temperature. The average inlet temperature for Run 1 was 35.7°C compared with 32.1°C for Run 8, a reduction of 3.6°C. The average DIL temperature was lowered by approximately 2.0°C over the bay temperature test range.

Fig 11 illustrates how average DIL temperature varied with bay temperature for Runs 1, 9, 10, 11 and 12, in which cold wall cooling only was used. The five curves represent a series of tests at the same total avionic power setting of approximately

138 W but with cooling air mass flowrate varying from 8.21×10^{-3} kg/s to 3.84×10^{-3} kg/s. It appears that there was a 'threshold level' of approximately 4×10^{-3} kg/s below which average DIL temperature was substantially affected by airflow while above this value the effects on temperature were less marked. Thus the DIL temperatures in Run 12, where the cooling air mass flowrate was below this 'threshold level', exhibited a significant increase over the whole bay ambient temperature range. This is more clearly depicted in Fig 12, which shows how the average DIL temperature varied with cooling air mass flowrate at various bay (ambient) temperatures.

Fig 13 shows the variation of cold wall heat pick-up with cooling air mass flowrate, while Fig 14 is a carpet plot showing the influence of cooling air mass flowrate and bay temperature on cold wall heat pick-up expressed as a percentage of the total avionic power.

Fig 14 shows clearly that the heat removal by the cold wall is much more sensitive to cooling air mass flowrate at higher bay temperatures. Again there is a marked reduction in cold wall effectiveness below about 4×10^{-3} kg/s.

Run 13 was intended to investigate the effect of removing the insulation from beneath the electronic equipment (adjacent to the cold wall) thus allowing heat loss/gain to the bay. The polystyrene block, on which the avionic box stood within the chamber, was removed and replaced by four small Tufnol blocks to allow air movement beneath the equipment. The results are shown in Figs 15 and 16 which show respectively, average DIL temperatures and the heat flowrate to the cold wall as a function of bay (ambient) temperature. In each case the results of Run 1 are included for comparison. It is evident from Fig 15 that at low bay temperatures, exposing the cold wall to the bay ambient air (Run 13) is beneficial, resulting in slightly lower average DIL temperatures. At higher ambient temperatures however, the reverse is true. Fig 16 reveals how exposure of the cold wall lower surface has affected heat pick-up by the wall. In comparison with Run 1 additional heat pick-up begins at approximately 38°C and increases at higher bay temperatures to about a 21 W increase at 70°C. In a practical situation with equipments being cooled sequentially, *ie* along a cold plank, the accumulative heat pick-up from the bay and consequent increase in component temperatures may well reveal a need to insulate the cold wall/plank from the surroundings.

Wherever an avionic box is situated, the temperature of the surroundings is likely to influence component temperatures to some degree. In order to assess that influence (*ie* heat pick-up or rejection from the test chamber to the avionic box) the avionic box was completely encased in a purpose built expanded polystyrene jacket and operated at full avionic power (nominally 138 W) over a bay (ambient) temperature range of 25.5°C to 58.0°C (Run 14). The variation of average DIL temperature with bay temperature for Run 14 is shown in Fig 15. Clearly the insulation was not perfect, hence the slight increase in DIL temperature with increasing ambient temperature. In comparison with Run 1 (same power but no insulation) the effect of reduced heat rejection to the surrounding bay at low to mid-range ambient temperatures is most evident. At higher bay (ambient) temperatures, *ie* approximately 65°C and above, the DIL temperatures in the

uninsulated box would be higher than those in the insulated box. In practice, excessive bay temperatures may occur occasionally, to the detriment of the avionics. However, if the equipment is insulated, the advantage of heat rejection to the bay under less severe conditions would be lost. A further serious disadvantage resulting from insulating the avionics would be that equipment would be very vulnerable to loss of air supplies which would cause component temperatures to rise rapidly and soon lead to failure. Hence insulating the avionics should only be considered when equipment would have to operate in a very hot environment for most of the time but in all other circumstances insulation should be omitted.

Figs 17 to 21 are a series of graphs which show how the temperature difference between certain components and the cold plate (immediately below) varied with cooling air mass flowrate at various bay temperature levels. Fig 17 shows how the temperature of the hottest DIL of those instrumented (*ie* Channel 15 on PCB VII Fig 6) varied with cooling air mass flowrate through the cold wall. Clearly there is an increase in temperature difference (and hence heat conduction) with increasing flowrate. Fig 17 also shows the effect of bay (ambient) temperature variation. The hottest DIL referred to was situated in the uppermost position on the instrumented rung of the copper ladder. At the base of the same rung (on which a total of five DILs were mounted) was another DIL of identical type operating at the same voltage (see Fig 6). Fig 18 is similar to Fig 17 showing how the temperature difference between this lower positioned DIL and the cold plate varies with cooling air mass flowrate at various ambient temperatures. Comparison indicates that the DIL nearest the cold wall was always operating at lower temperatures. For example, at 70°C bay temperature the lower placed DIL was operating between 10-13°C (approximately) cooler, depending on the flowrate. Furthermore the lower component was noticeably less sensitive to changes in ambient temperature. The latter point is illustrated in Fig 19 where actual DIL temperatures were plotted against cooling air mass flowrate.

The DILs referred to above were both mounted on PCB VII which was positioned close to the power supply unit towards the cooling air exit side of the avionic box. Curves similar to those in Figs 17 and 18 have been drawn for two of the DILs mounted on PCB III (*ie* Figs 20 and 21 which correspond to DILs on channels 5 and 9 respectively - see Fig 6). Unlike PCB VII where the DILs referred to were on an outer copper ladder rung close to the front face of the avionic box, the instrumented DILs on PCB III were on the central rung (see Fig 6) and PCB III itself was positioned close to the cooling air inlet side of the avionic box.

A comparison of Figs 20 and 21 again shows that the lower DIL benefits from lower operating temperature and reduced sensitivity to changes in ambient (bay) temperature.

All DILs mounted on the two PCBs closest to the cooling air inlet (PCB XV and XVI) were cooled using an aluminium alloy interplate. The plate was sandwiched between the two boards, which were lightly bolted together so ensuring contact between the top surfaces of the DILs and the interplate. The interplate connected the roof of the box

with the cold wall, the ends of the interplate being fitted into grooves machined into the raised sections of the upper and lower PCB guides.

Fig 6 shows the PCB layout within the avionic box and the position of individual components on each PCB. The centre column of components on PCBs I and XV were of the same type, *ie* Beckman resistors, the former utilising copper ladder heat conduction to the cold wall, the latter being similarly cooled using the alloy interplate. Although both PCBs were operated at a similar voltage and power level, to permit comparison of the two methods of cooling, PCB XV power was taken as the mean of the two boards cooled by the interplate. Correction was then made for the difference in power dissipation between PCB XV and PCB I. The corrected results from Run 1 were used to produce Figs 22 and 23.

Fig 22 shows how the temperature of each DIL in the centre column of components on PCBs I and XV (relative to the cold plate directly below) varied with bay temperature. The graphs show that the interplate cooled DILs situated either close to the cold wall or near the avionic box roof, are likely to operate at a similar temperature to comparable copper ladder cooled DILs. However, the interplate cooled DILs around the mid-height position revealed a significant reduction in operating temperature compared with the copper ladder cooled components, particularly at lower bay temperatures. For example, at a bay temperature of 30°C the ΔT (DIL temperature-cold plate temperature) for the interplate cooled DIL at the mid-height position was approximately 7°C lower, although at the higher bay temperature of 70°C this figure was reduced to about 4°C.

Fig 23 illustrates how DIL temperature (relative to the cold plate) varied with DIL positions, *ie* their position in the vertical column of five DILs. Once again the central interplate cooled components were seen to be operating at a lower temperature than those mounted on the copper ladder. The slightly concave shape of the interplate curves (convex for the copper ladder curves) is not easily explained. It might well be due to the rather basic method by which PCBs XV and XVI were clamped to the interplate. As stated above, the PCBs were positioned on each side of the interplate and were simply bolted together along their two vertical sides. This may have caused the glass fibre PCBs to have bowed, therefore reducing the contact area between DIL case(s) and interplate with a resultant increase in thermal resistance. Indeed the latter suggests that any reduction in DIL temperatures as indicated by Figs 22 and 23 may well be a conservative estimate of any benefit interplate cooling may provide.

It perhaps should be mentioned that the weight of the interplate compared reasonably well with that of the copper ladder. The 180mm × 152mm × 1.6mm thick interplate weighed 120 g, *ie* 60 g per PCB cooled, the copper ladder weighed 52 g.

6 CONCLUSIONS

(1) Over the bay (ambient) temperature range investigated (20-70°C approximately) average DIL temperature increased (almost linearly) with increasing bay temperature.

(2) Operation of the avionic equipment in the inverted position resulted in a minimal change of average DIL temperature.

(3) Heat conduction to the cold wall via the metal sides of the avionic box was negligible.

(4) Attachment of a finned plate to the top surface of the avionic box reduced the average DIL temperature by approximately $2^{o}C$, in conditions of near-natural convection.

(5) While operating at maximum avionic power (138 W), circulation of cold wall outlet air through the avionic box (mixed air-wash) lowered the average DIL temperature approximately $11^{o}C$ over the entire bay (ambient) temperature test range.

(6) Whilst maintaining approximate ARINC 404A standard flowrate conditions ($21.8\ kg\ h^{-1}\ 100\ W^{-1}$), operation of the avionics at reduced total power resulted in a lowering of average DIL temperature.

(7) A reduction in cold wall inlet temperature produced a corresponding decrease in average DIL temperature.

(8) Decreasing the cooling air mass flowrate to the cold wall increased average DIL temperature, the effect became increasingly important for flowrates below 4×10^{-3} kg/s.

(9) Average DIL temperature was slightly reduced by exposure of the cold wall lower surface at low bay (ambient) temperature, the converse was so at high bay temperature.

(10) Avionic box insulation is of benefit only when frequent or continuous operation in a hot environment is required.

(11) A copper ladder mounted DIL will operate at lower temperature and exhibit less variation with ambient temperature, the closer it is to the cold wall.

(12) DILs situated close to the cold wall or the avionic box roof will operate at similar temperatures whether cooled using an alloy interplate or a copper ladder.

(13) DILs positioned centrally within the avionic box will operate at a lower temperature if interplate rather than copper ladder cooled.

Table 1

SUMMARY OF TEST RESULTS

Run No.	Bay (ambient) temperature (°C)	Inlet temperature (°C)	Outlet temperature (°C)	Total avionic power (W)	Power supply unit (W)	Heat flow-rate to cold wall (W)	Indicated cooling air volumetric flowrate Rotameter ($m^3/s \times 10^3$)	Cooling air mass flowrate ($kg/s \times 10^3$)	Average DIL temperature (°C)	Maximum DIL temperature (°C)	Average internal ambient (°C)	Side walls	Finned top plate	Box position	Remarks (mixed air-wash used only where stated)
1	23.0	35.6	43.5	138.7	32.0	67.5	6.89	8.22	66.9	77.8	65.6	Aluminium	None	Normal	Avionic box in normal position, this is regarded as the 'standard' test. Average cooling air mass flowrate of 8.21×10^{-3} kg/s.
"	40.0	"	46.8	138.0	"	95.6	"	"	71.0	82.2	68.8	"	"	"	
"	60.0	36.0	52.3	137.3	"	139.2	"	"	78.3	91.1	76.1	"	"	"	
"	70.0	35.6	55.1	137.0	"	165.4	6.84	8.17	82.4	96.8	80.1	"	"	"	
2	22.0	35.6	44.1	138.3	32.0	68.6	6.51	7.77	68.1	76.6	67.0	"	"	Inverted	Avionic box inverted.
"	40.0	"	48.6	136.7	31.0	104.9	"	"	72.9	82.5	71.2	"	"	"	
"	60.0	"	55.5	138.0	32.0	160.6	"	"	80.3	92.3	78.2	"	"	"	
"	70.0	36.3	59.0	136.4	31.0	183.2	"	"	84.9	97.4	82.8	"	"	"	
3	23.0	35.7	44.0	138.4	32.0	69.0	6.75	8.05	66.9	77.6	65.3	Bakelite	"	Normal	Bakelite side walls fitted.
"	70.0	35.8	54.7	136.6	32.0	161.4	6.89	8.22	82.3	97.0	79.7	"	"	"	
4	24.0	35.3	42.6	139.1	32.0	63.6	7.03	8.39	64.0	72.9	62.9	"	Fitted	"	Bakelite side walls plus finned top plate.
"	42.0	36.0	46.6	138.6	"	91.7	6.99	8.33	69.7	80.0	67.9	"	"	"	
"	60.0	35.6	51.0	137.8	"	132.4	6.94	8.28	76.9	89.0	74.9	"	"	"	
"	69.0	35.6	53.4	137.3	"	153.0	6.94	8.28	80.7	94.2	78.3	"	"	"	
5	23.0	35.9	42.4	137.9	31.0	54.4	6.75	8.05	56.1	63.5	54.0	Aluminium	None	Normal	Introduction of mixed air-wash (*ie* air-wash plus conduction/cold wall cooling). Aluminium side walls.
"	47.0	35.6	46.5	137.4	31.0	89.2	6.61	7.88	62.3	69.2	60.3	"	"	"	
"	60.0	35.6	50.2	137.8	32.0	117.8	6.51	7.77	67.5	75.0	65.4	"	"	"	
"	70.0	35.5	52.9	137.6	32.0	142.5	6.61	7.88	71.3	79.3	69.8	"	"	"	
6	24.0	35.6	41.2	110.8	31.0	40.3	5.81	6.93	52.1	58.5	50.4	"	"	"	Avionic power reduction plus mixed air-wash.
"	46.0	35.8	46.3	111.2	32.0	74.9	5.76	6.87	58.4	63.6	57.2	"	"	"	
"	60.0	36.0	51.2	109.7	31.0	107.6	5.71	6.81	64.7	71.3	63.7	"	"	"	
"	70.0	35.8	54.9	110.7	32.0	135.2	5.71	6.81	69.8	77.1	68.7	"	"	"	
7	23.0	35.8	43.0	111.9	32.0	48.8	5.48	6.53	59.0	67.7	57.4	"	"	"	Avionic power reduction.
"	50.0	35.4	49.8	111.4	"	96.8	5.43	6.48	66.1	76.3	64.6	"	"	"	
"	61.0	35.8	54.4	110.9	"	124.0	5.38	6.42	72.1	82.9	69.4	"	"	"	
"	69.0	35.8	57.0	110.5	"	140.1	5.33	6.36	75.2	87.7	72.6	"	"	"	
8	23.0	32.0	40.5	138.3	31.0	69.6	6.61	7.88	64.2	75.2	62.6	"	"	"	Inlet temperature reduction.
"	44.0	32.0	44.7	137.4	"	103.2	6.56	7.83	70.2	82.7	68.2	"	"	"	
"	60.0	32.2	49.2	136.8	"	139.2	6.61	7.88	75.9	89.7	73.4	"	"	"	
"	69.0	32.2	52.0	135.6	"	162.1	6.61	7.88	80.1	95.1	77.4	"	"	"	

Table 1 (concluded)

Run No.	Bay (ambient) temperature (°C)	Inlet temperature (°C)	Outlet temperature (°C)	Total avionic power (W)	Power supply unit (W)	Heat flowrate to cold wall (W)	Indicated cooling air volumetric flowrate Rotameter ($m^3/s \times 10^3$)	Cooling air mass flowrate ($kg/s \times 10^3$)	Average DIL temperature (°C)	Maximum DIL temperature (°C)	Average internal ambient (°C)	Side walls	Finned top plate	Box position	Remarks (mixed air-wash used only where stated)
9	22.5	35.4	44.2	137.3	30.0	64.8	5.95	7.10	66.9	77.8	65.4	Aluminium	None	Normal	Average cooling air mass flowrate reduced to 7.10×10^{-3} kg/s.
"	46.0	"	49.0	137.3	31.0	100.2	"	"	73.0	85.1	71.0	"	"	"	
"	54.0	"	52.0	137.1	"	122.3	"	"	76.5	89.5	74.1	"	"	"	
"	68.0	"	55.7	136.3	"	149.6	"	"	81.8	96.2	79.1	"	"	"	
10	27.0	35.8	47.2	137.8	31.0	74.0	5.24	6.23	69.5	80.2	68.1	"	"	"	Average cooling air mass flowrate reduced to 6.24×10^{-3} kg/s.
"	49.0	35.6	52.1	137.9	32.0	108.1	5.29	6.29	75.4	87.5	73.4	"	"	"	
"	60.0	35.6	56.0	137.5	32.0	132.4	5.24	6.25	80.2	93.4	77.9	"	"	"	
"	69.0	36.0	59.6	136.1	31.0	151.8	5.19	6.18	84.3	98.0	81.5	"	"	"	
11	27.5	35.4	49.0	137.8	31.0	71.6	4.25	5.05	70.3	81.3	68.6	"	"	"	Average cooling air mass flowrate reduced to 5.04×10^{-3} kg/s.
"	51.0	35.6	55.3	137.0	31.0	102.5	4.20	5.01	77.3	89.5	75.1	"	"	"	
"	58.5	"	58.6	135.9	30.0	121.1	4.25	5.07	81.4	94.4	78.8	"	"	"	
"	69.5	"	62.9	134.8	31.0	142.1	4.20	5.02	85.0	98.9	82.2	"	"	"	
12	26.5	35.4	51.9	136.6	30.0	65.6	3.21	3.85	71.7	82.3	69.8	"	"	"	Average cooling air mass flowrate reduced to 3.84×10^{-3} kg/s.
"	54.0	35.6	62.5	135.7	"	107.0	"	3.84	81.8	93.8	79.4	"	"	"	
"	62.5	35.6	67.4	135.6	"	126.5	"	3.84	86.5	99.5	83.9	"	"	"	
13	21.5	35.2	42.5	139.2	32.0	62.3	6.89	8.24	66.0	77.1	64.7	"	"	"	Bay (ambient) air circulation beneath cold wall.
"	47.0	35.6	48.7	138.6	"	112.6	6.94	8.28	73.2	85.7	71.1	"	"	"	
"	54.0	"	51.4	138.3	"	135.8	6.94	8.27	76.4	89.5	74.1	"	"	"	
"	67.5	"	56.2	137.7	"	178.3	6.99	8.33	82.1	96.7	79.3	"	"	"	
14	25.5	35.4	50.3	137.2	31.0	127.2	6.89	8.21	76.5	90.8	74.0	"	"	"	Insulated avionic box.
"	40.0	35.6	51.2	136.0	30.0	133.2	6.89	8.23	78.8	93.0	76.1	"	"	"	
"	52.0	35.4	52.5	136.0	30.0	145.0	6.84	8.18	80.4	95.4	77.7	"	"	"	
"	58.0	35.2	53.8	136.9	31.0	158.8	6.89	8.19	80.7	96.0	77.9	"	"	"	

REFERENCES

No.	Author	Title, etc
1	E.F. Swain	Aircraft avionics cooling present and future. NAECon '77 Record, pp 54-59 (1977)
2	E. Zara L. Midolo A. Mayer	Advanced environmental control for avionic systems. NAECon '77 Record, pp 60-67 (1977)
3	I.P. Gregory	Heat transfer from components mounted on different printed circuit boards within avionic equipments. RAE Technical Report 78060 (1978)

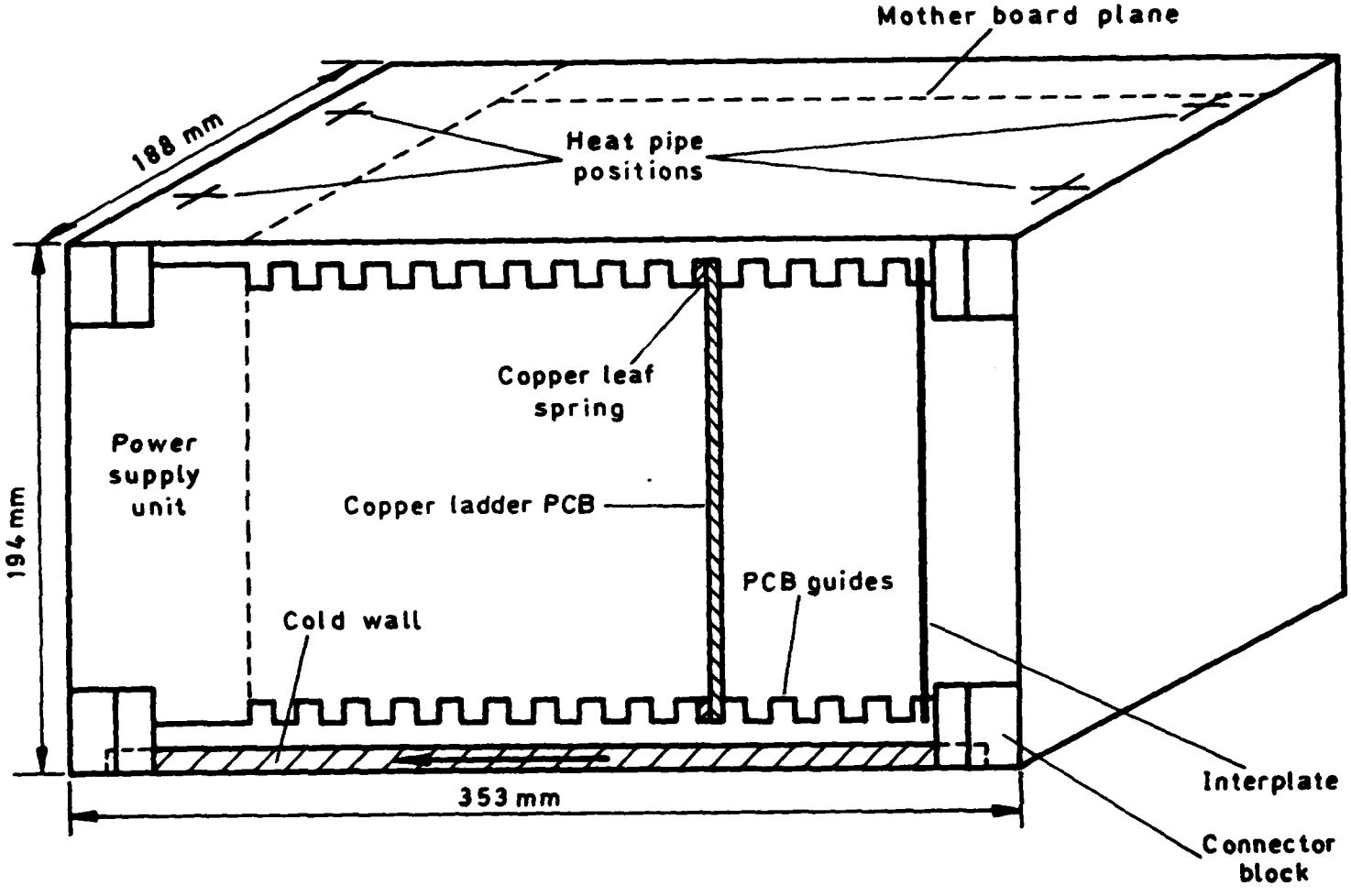

Fig 1 General layout and overall dimensions of the simulated avionic box

Fig 2

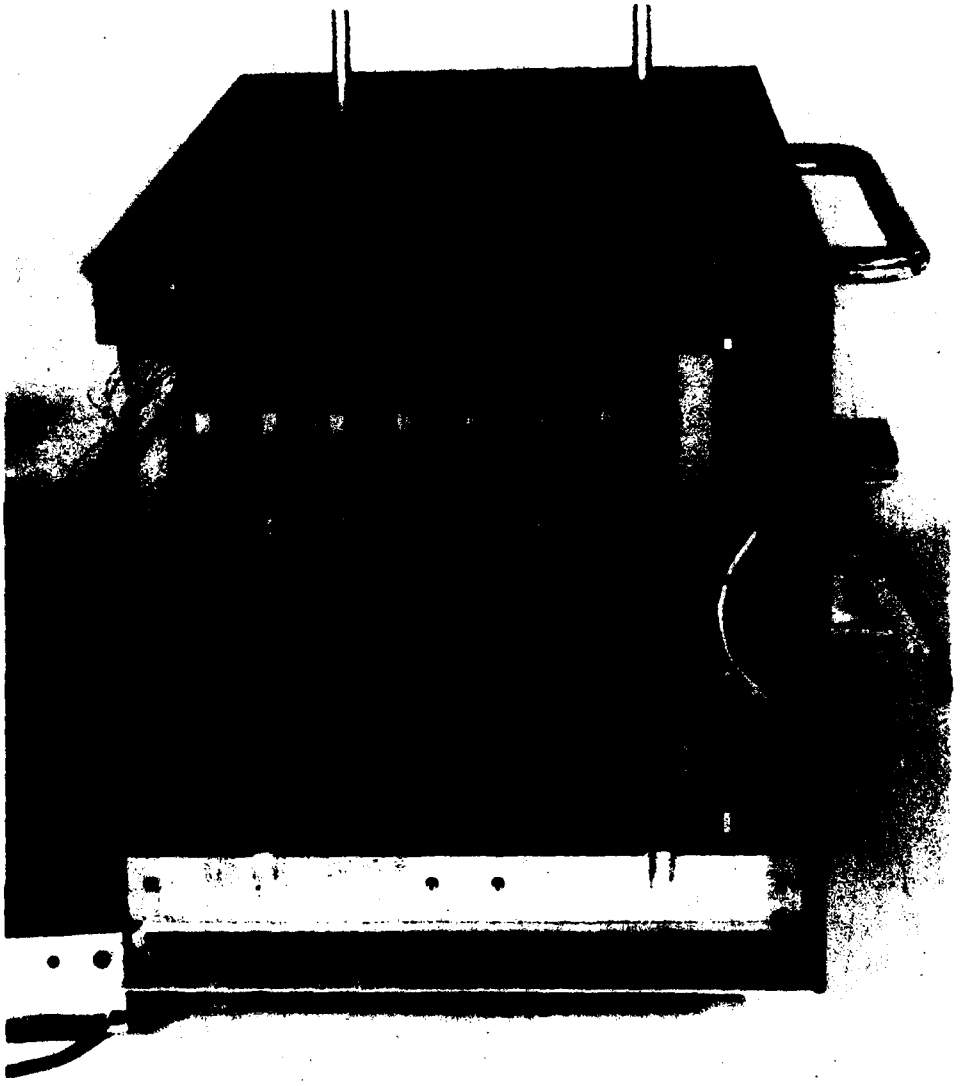

Fig 2 End view of the 'cold wall' heat exchanger (before 'interplate' was installed)

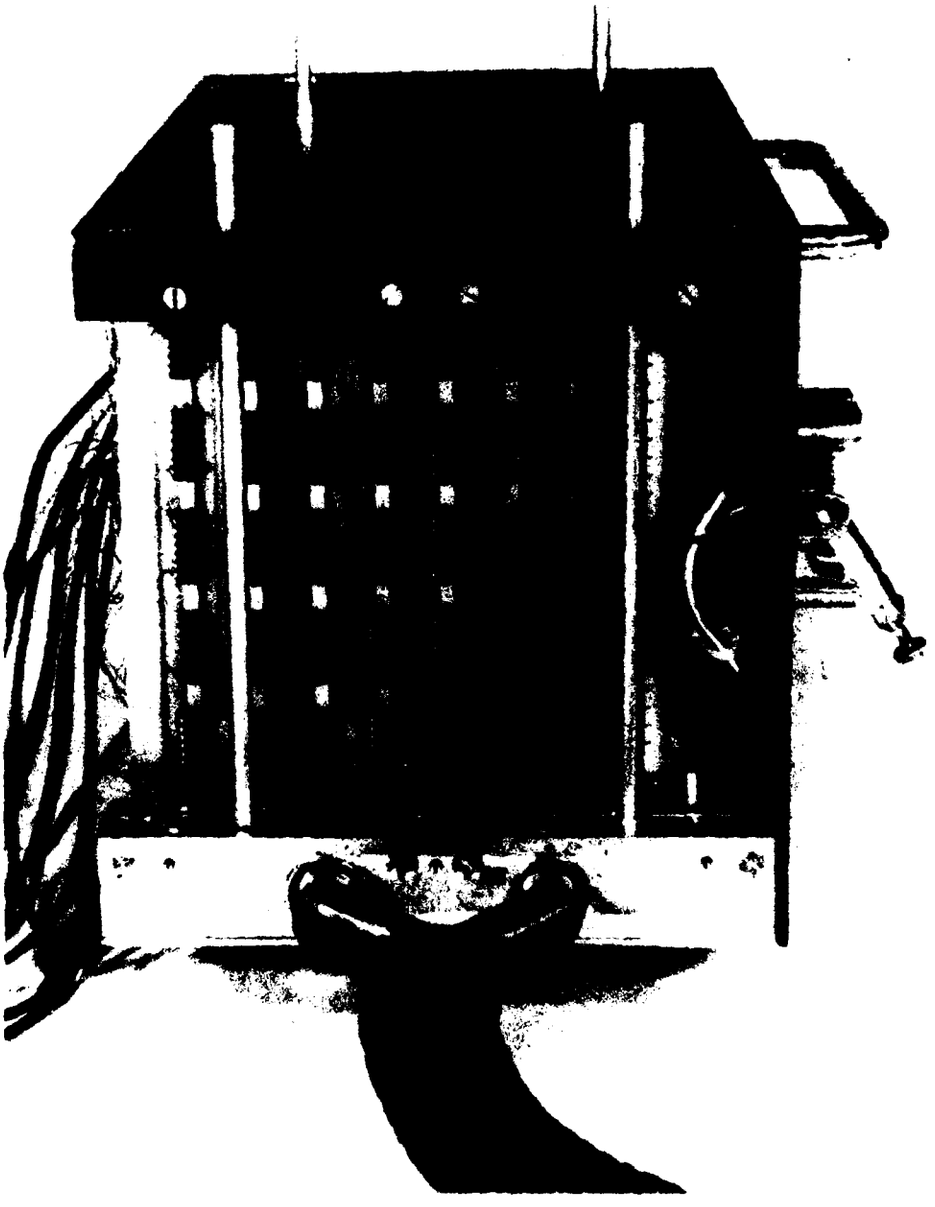

Fig 3 Y tube/connector block assembly (before 'interplate' was installed)

TR 82082 C17709

Fig 4 General layout within the simulated avionic box (front wall removed)

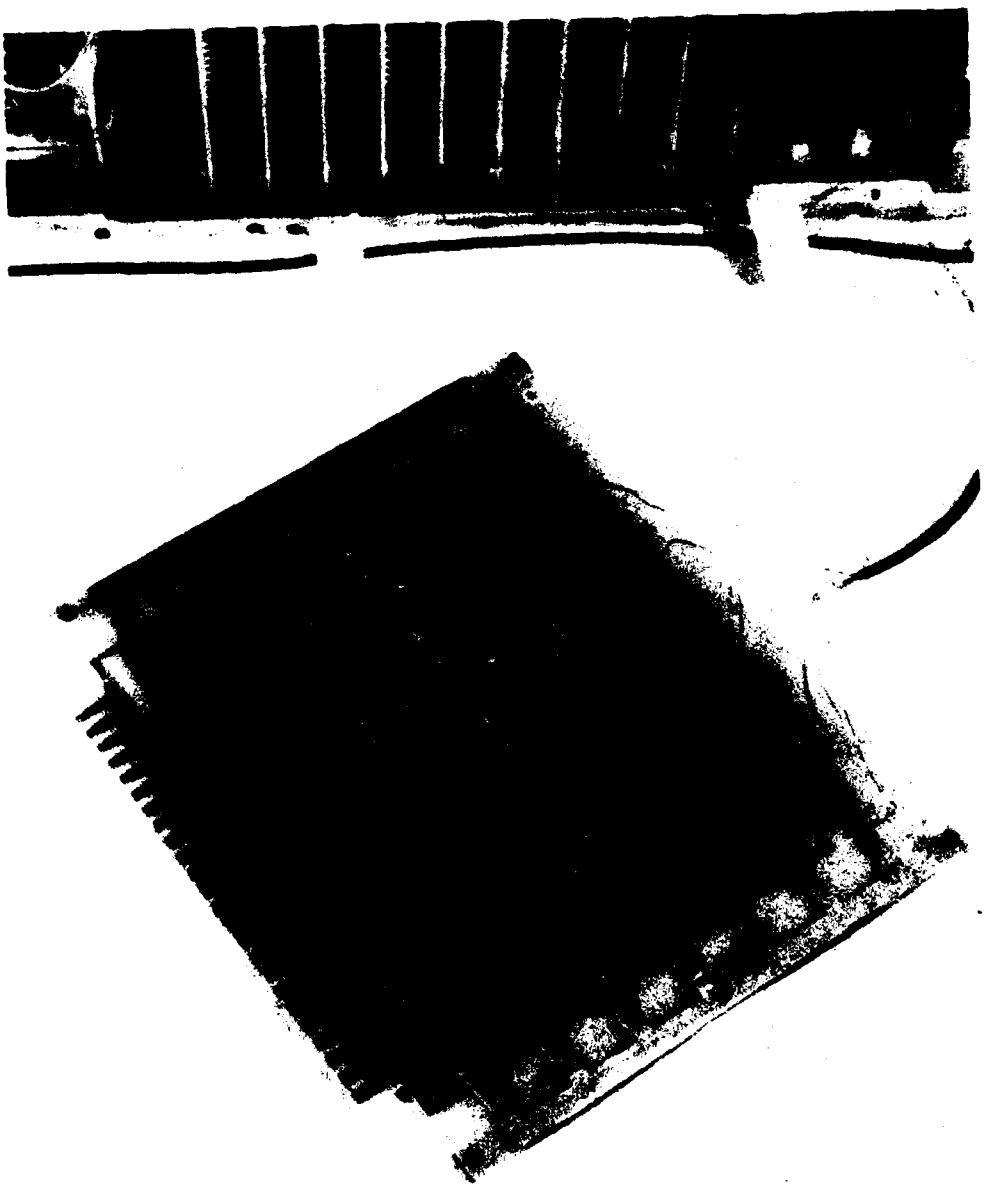

Fig 5 An instrumented copper ladder PCB

TR 8282 C17711

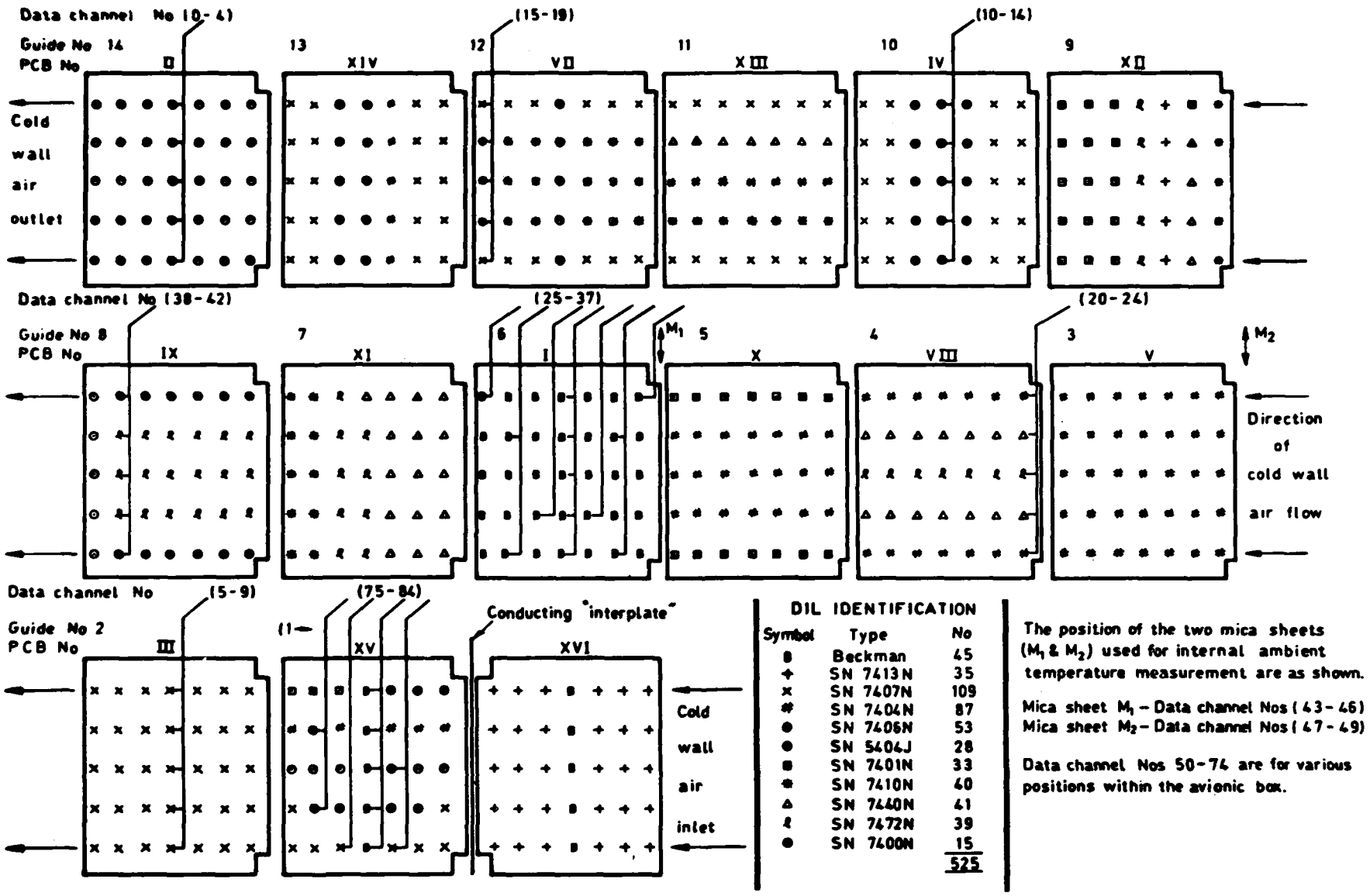

DIL IDENTIFICATION

Symbol	Type	No
■	Beckman	45
+	SN 7413N	35
×	SN 7407N	109
#	SN 7404N	87
●	SN 7406N	53
●	SN 5404J	28
■	SN 7401N	33
*	SN 7410N	40
△	SN 7440N	41
ℓ	SN 7472N	39
●	SN 7400N	15
		525

The position of the two mica sheets (M_1 & M_2) used for internal ambient temperature measurement are as shown.

Mica sheet M_1 – Data channel Nos (43-46)
Mica sheet M_2 – Data channel Nos (47-49)

Data channel Nos 50-74 are for various positions within the avionic box.

Fig 6 PCB and component layout (including instrumented DILs) within the avionic box

Fig 6

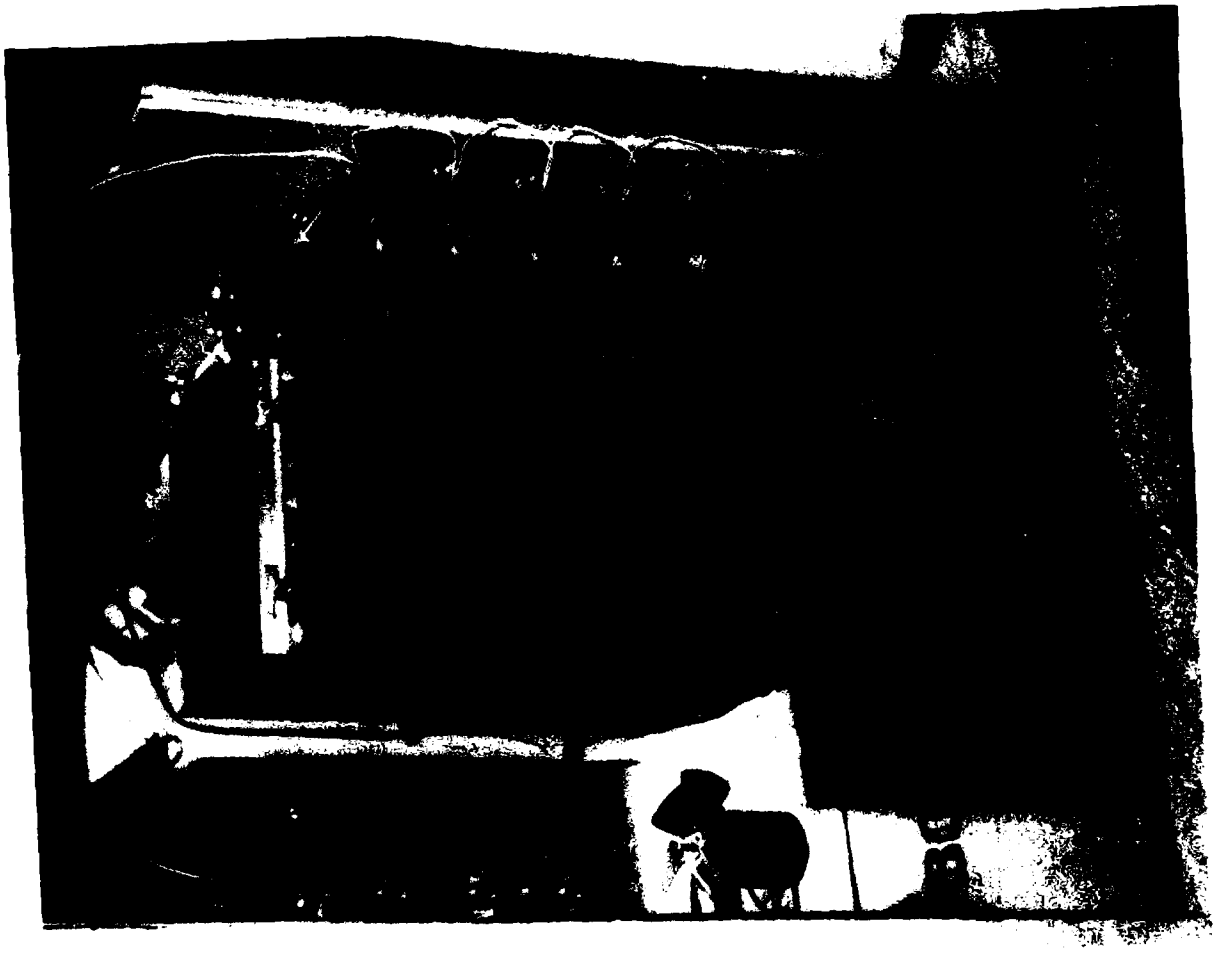

Fig 7 Simulated avionic box placed within test chamber (box front wall removed, air-wash inlet duct fitted to rear wall)

Fig 8

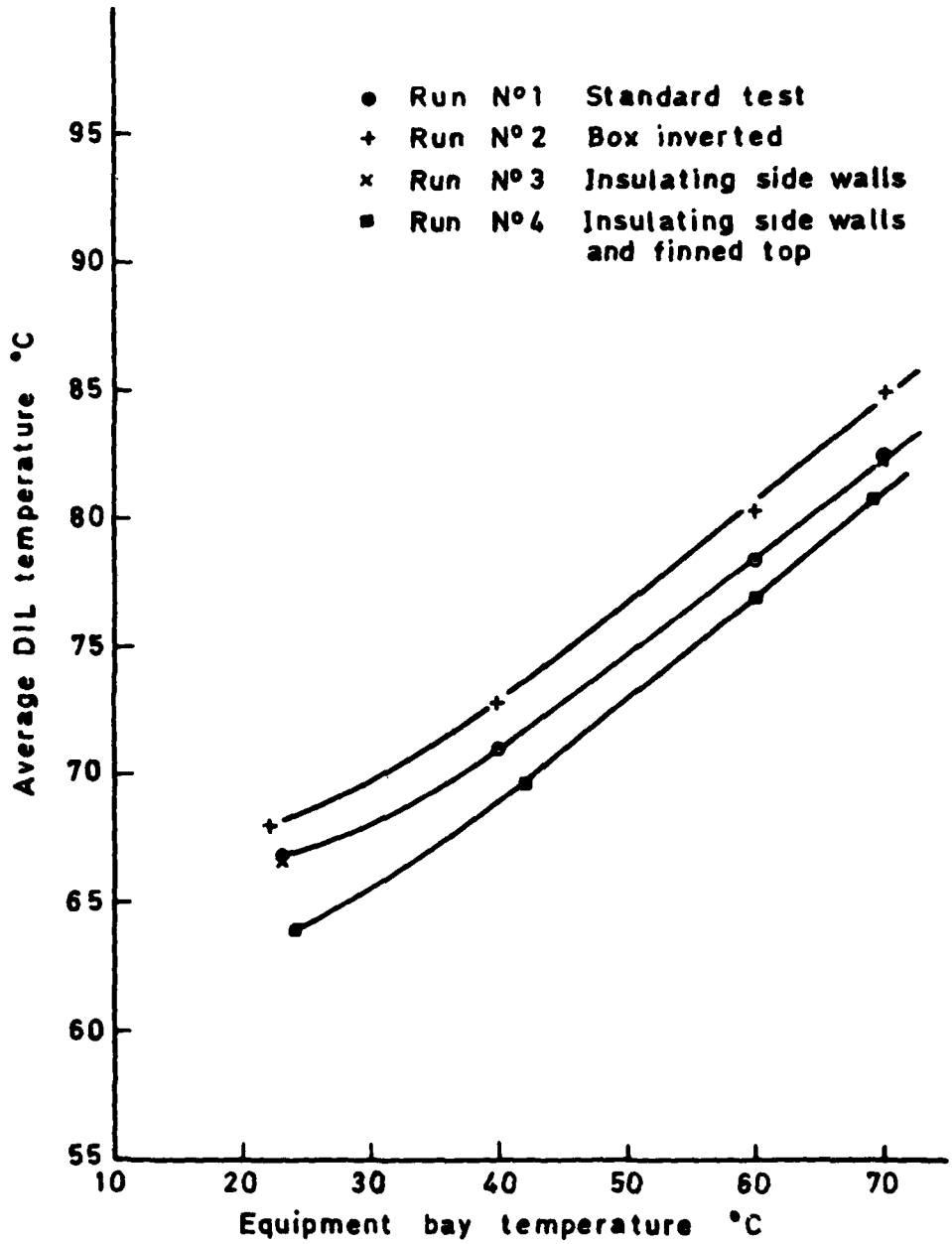

Fig 8 The effect on component temperatures of improved heat transfer from equipment top surface

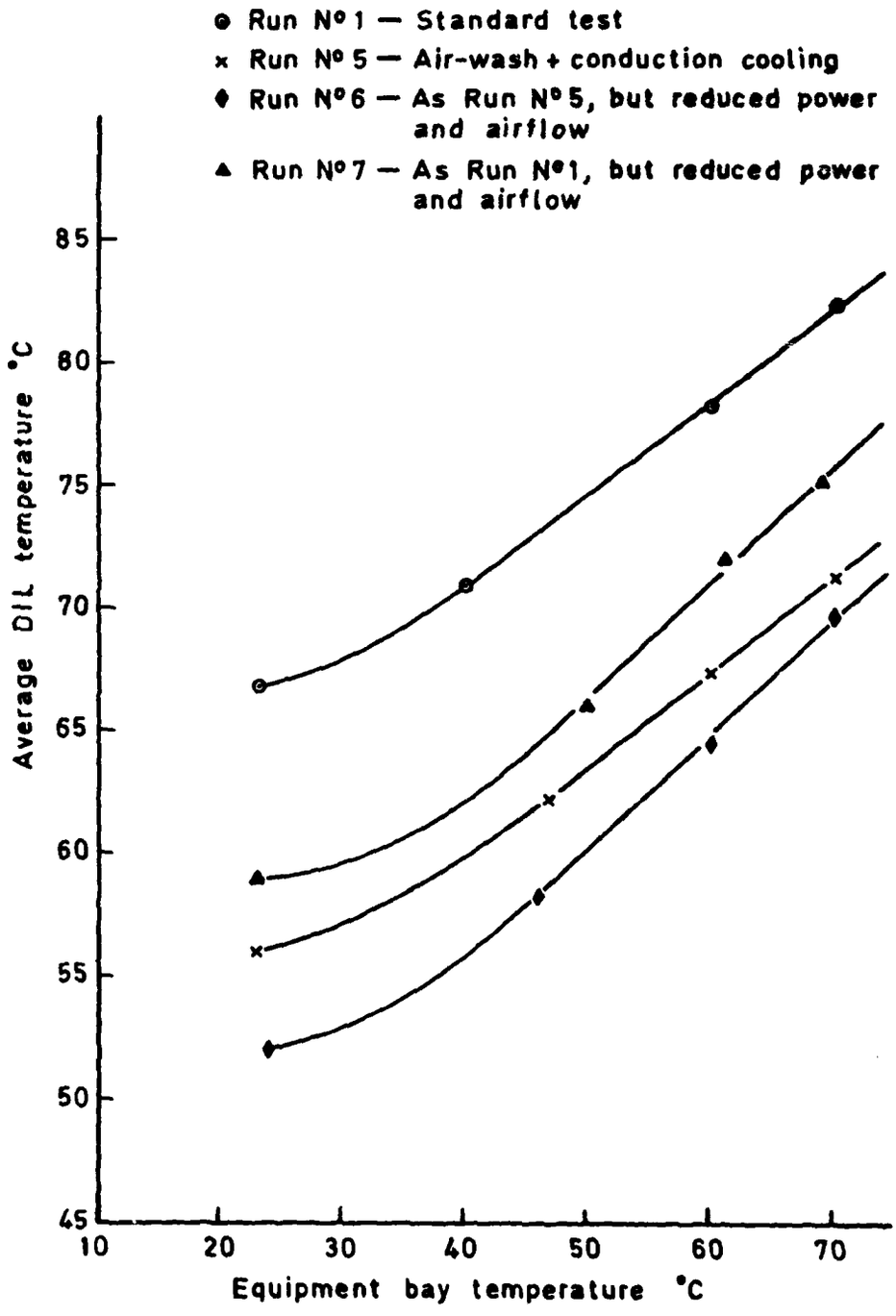

Fig 9 The effect of air-wash on component temperatures – at two power levels

Fig 10

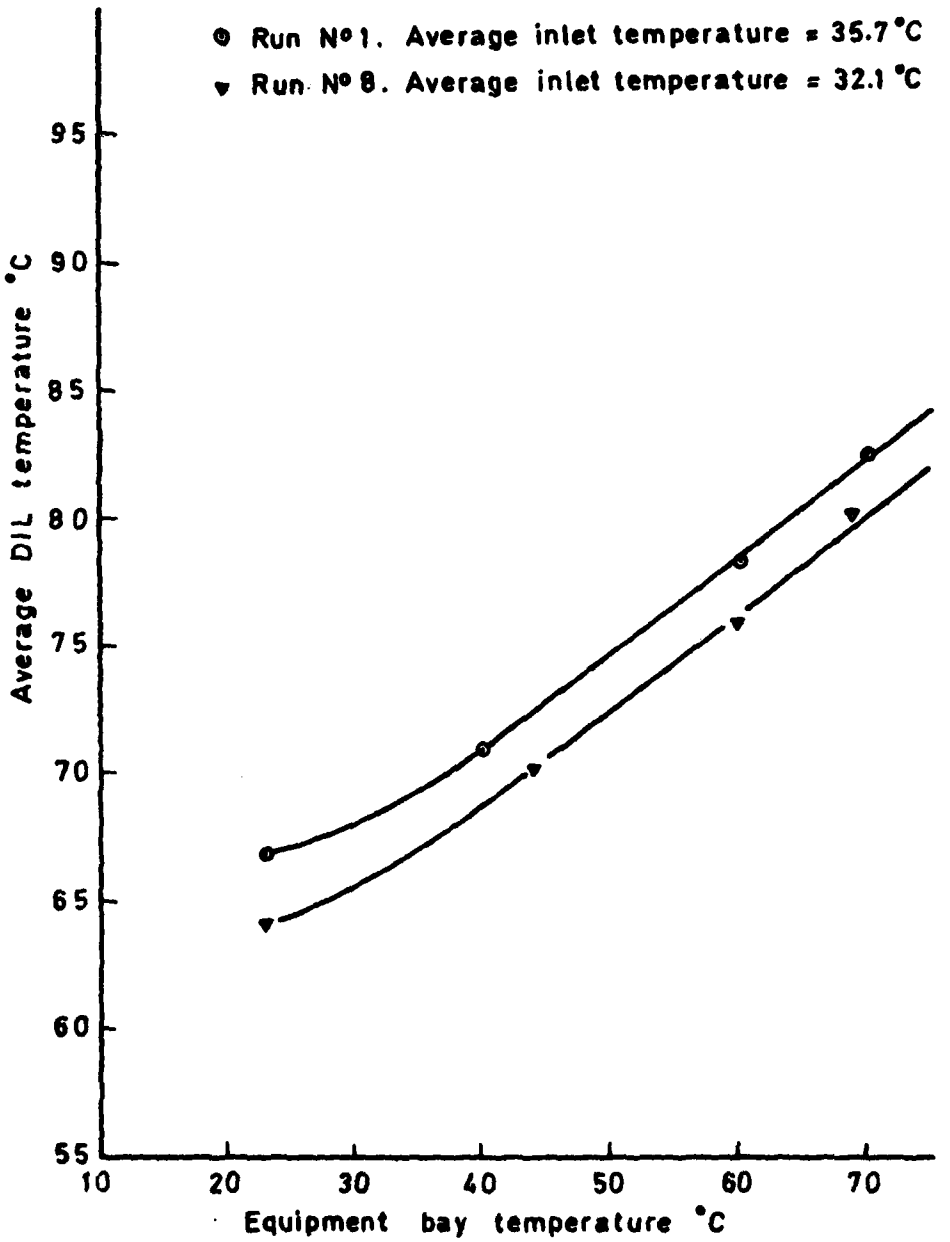

Fig 10 The effect of inlet air temperature on component temperatures

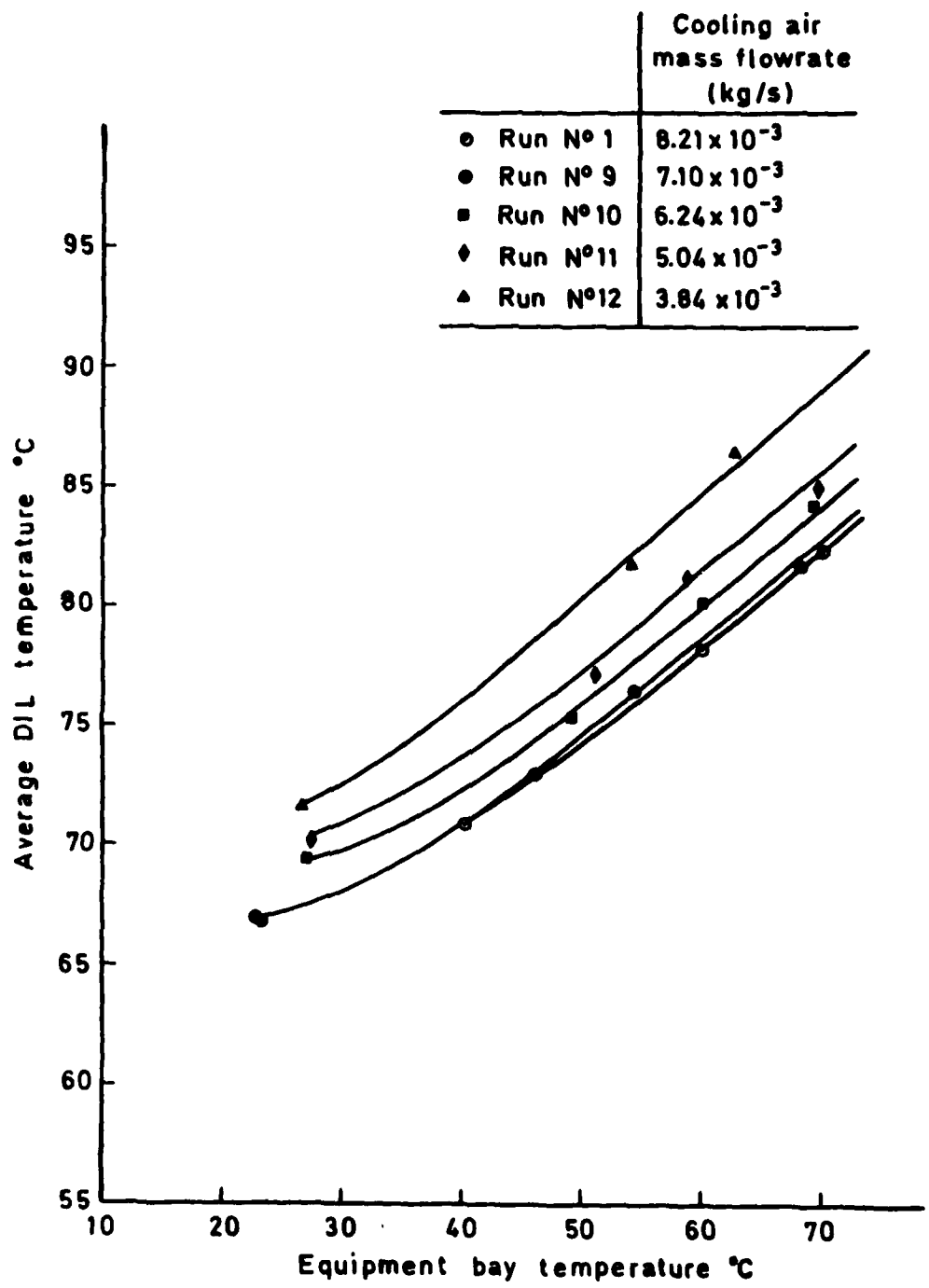

Fig 11 The effect of cooling air mass flowrate on component temperatures

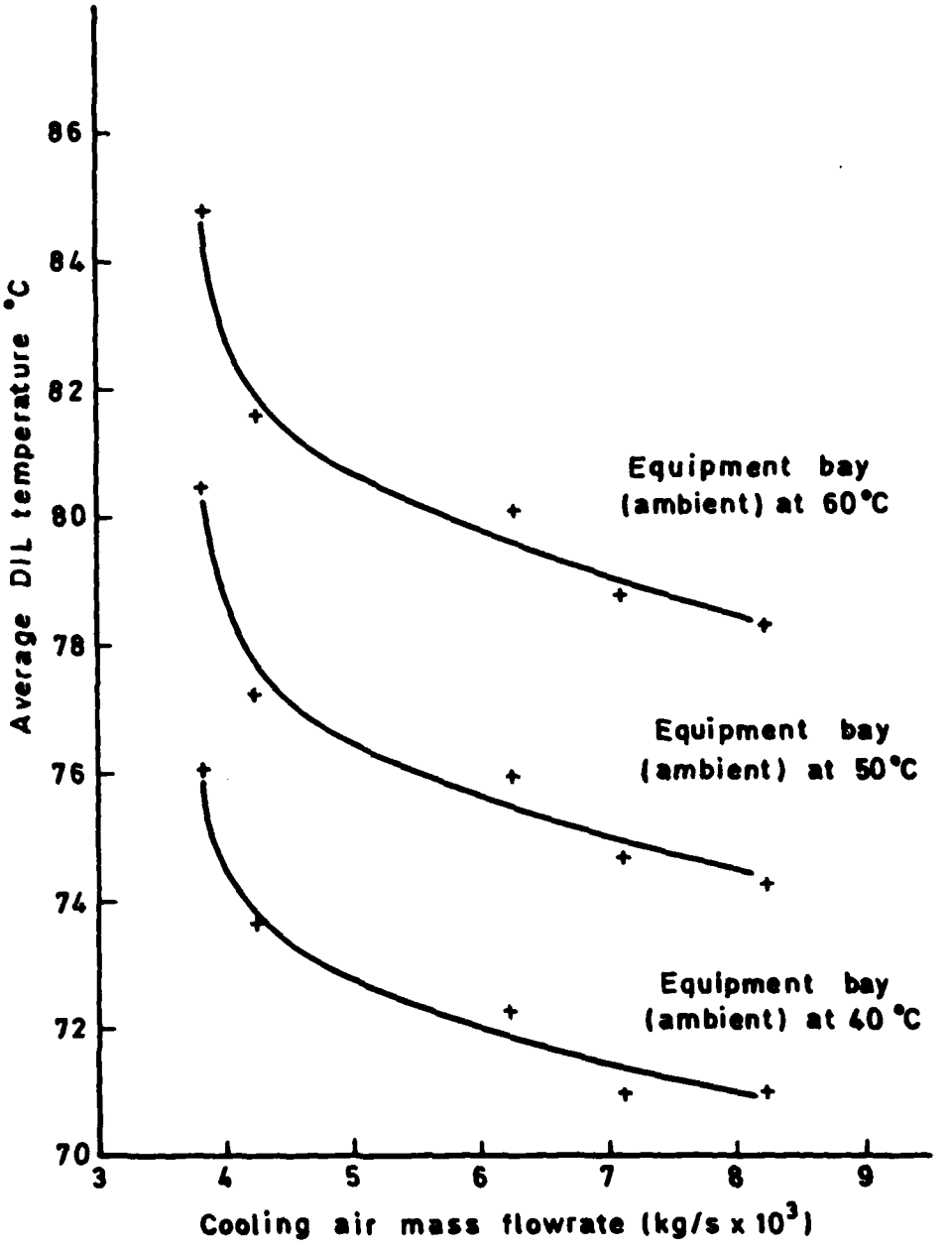

Fig 12 The effect of cooling air mass flowrate on component temperatures at constant equipment bay temperatures

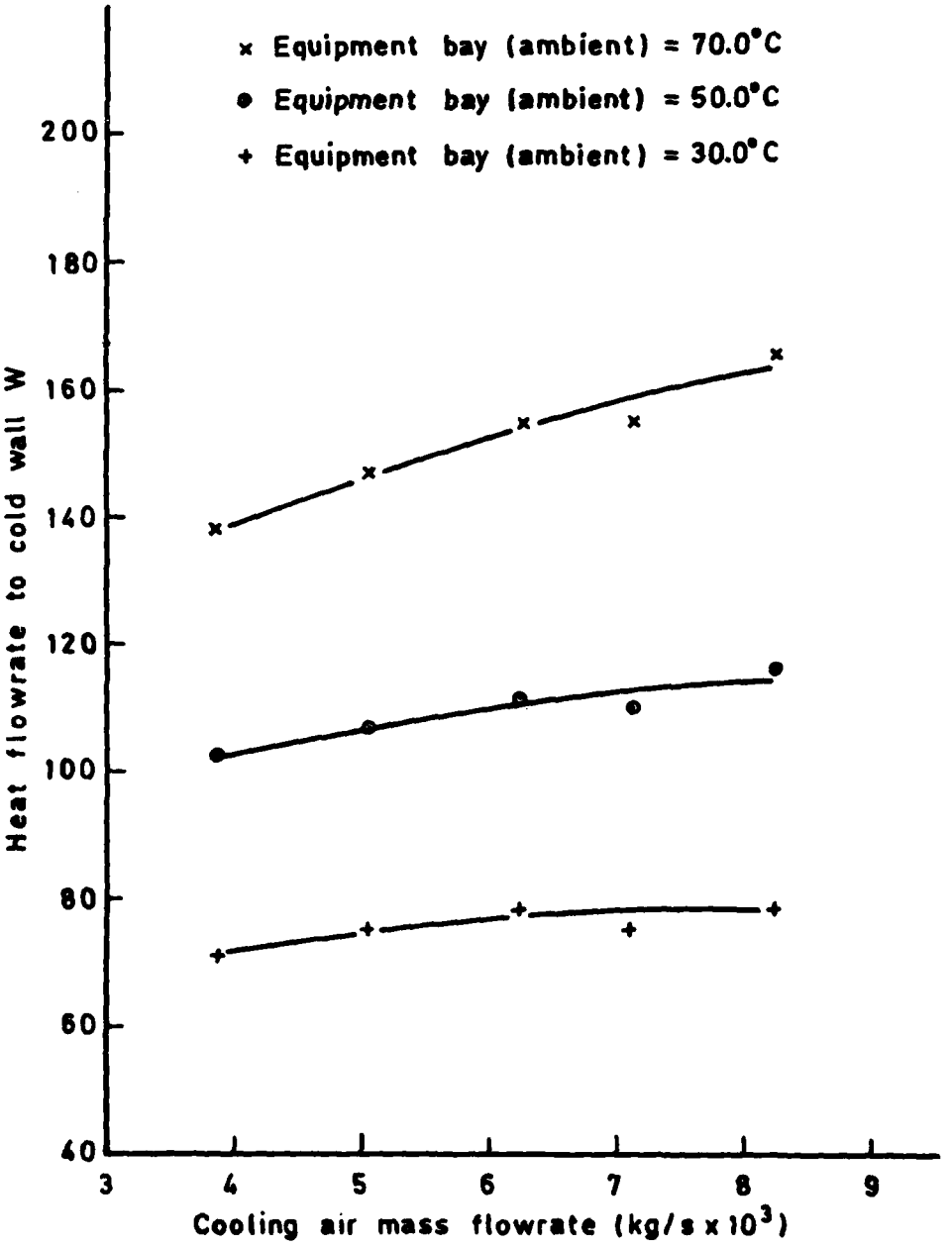

Fig 13 The effect of cooling air mass flowrate on cold wall heat pick-up

Fig 14

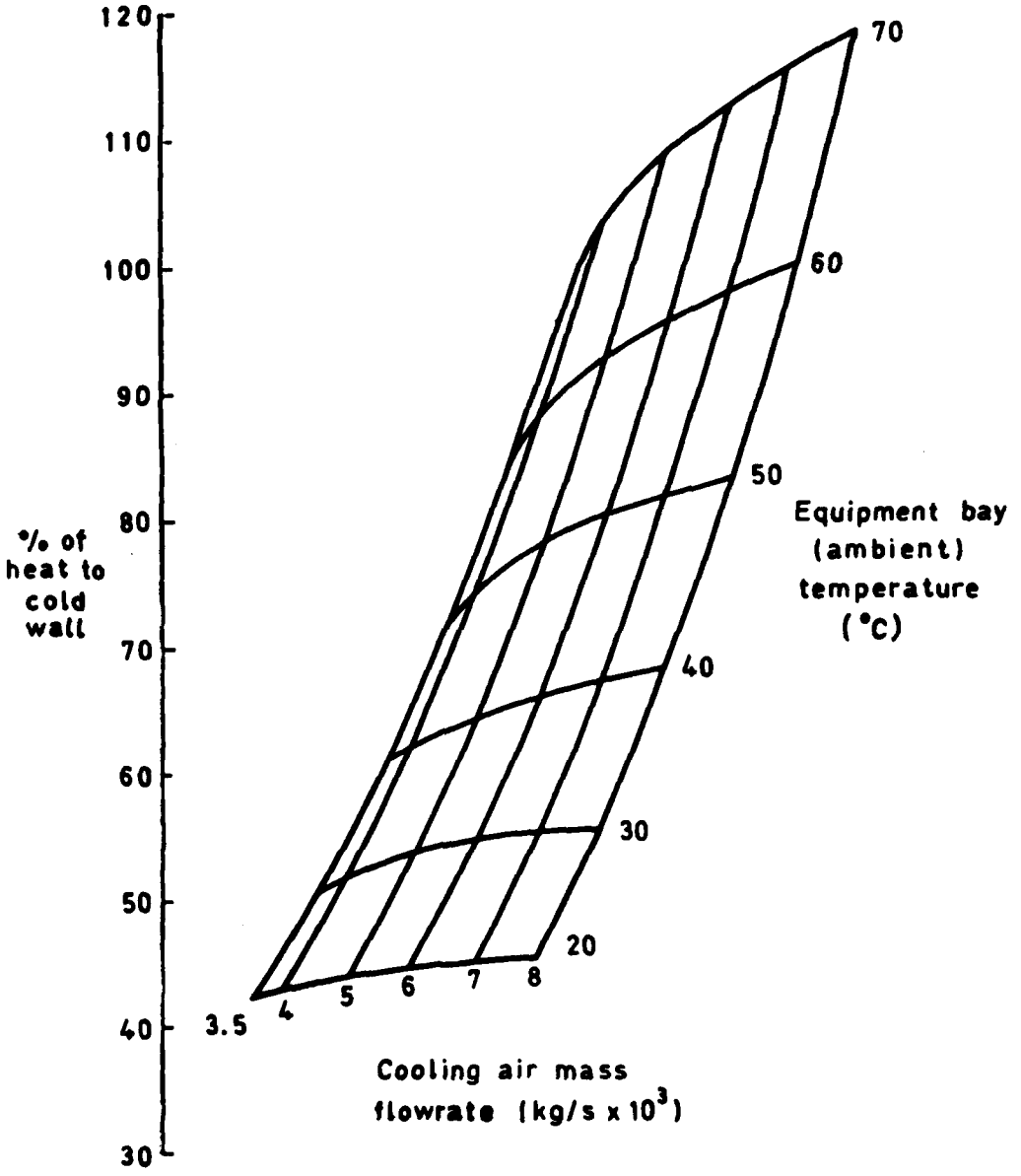

Fig 14 **The variation in cold wall heat pick-up with cooling air mass flowrate and equipment bay temperature**

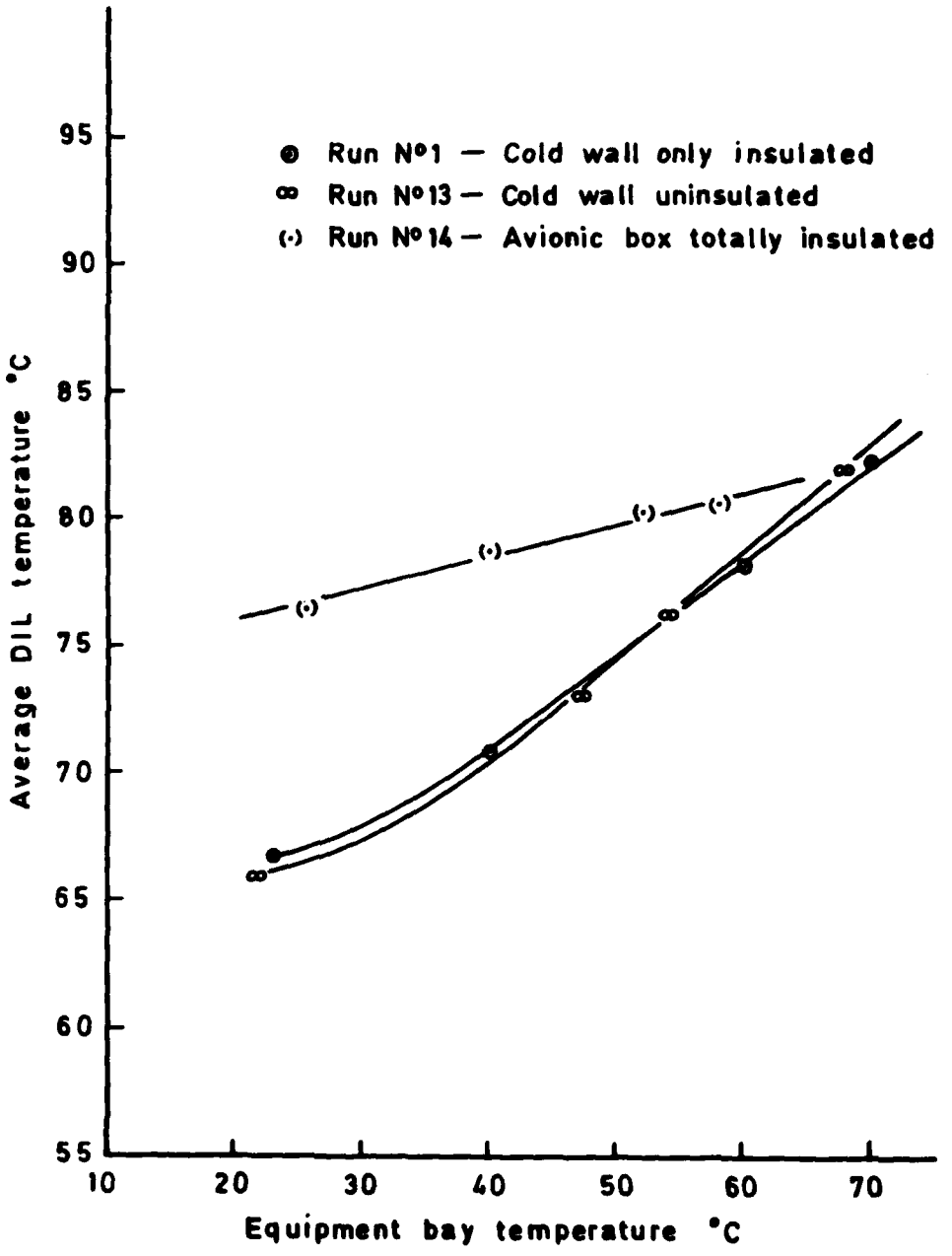

TR 82092

Fig 15 The effect of cold wall and avionic box insulation on component temperatures

Fig 16

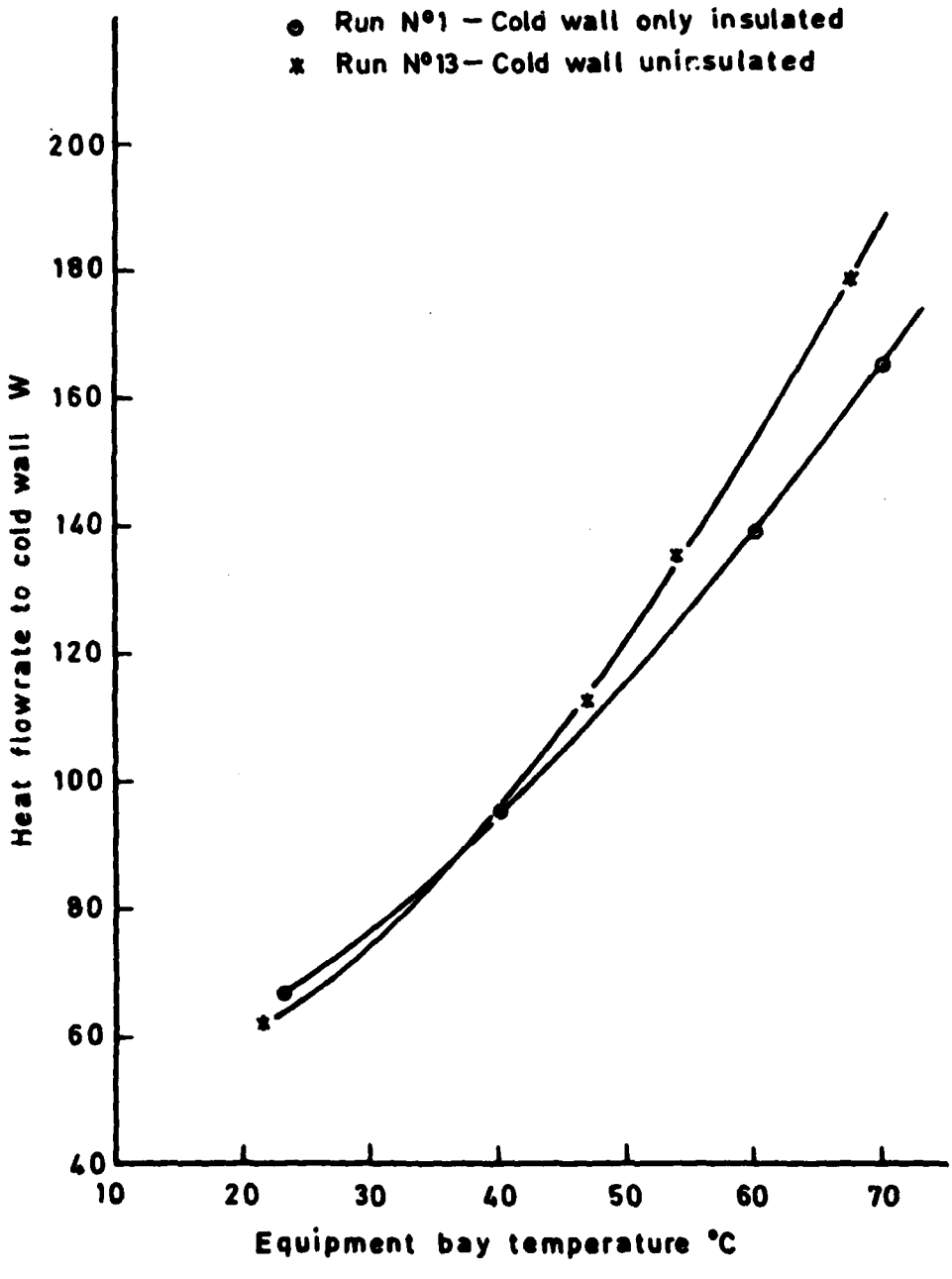

Fig 16 The effect of cold wall insulation on the cold wall heat extraction

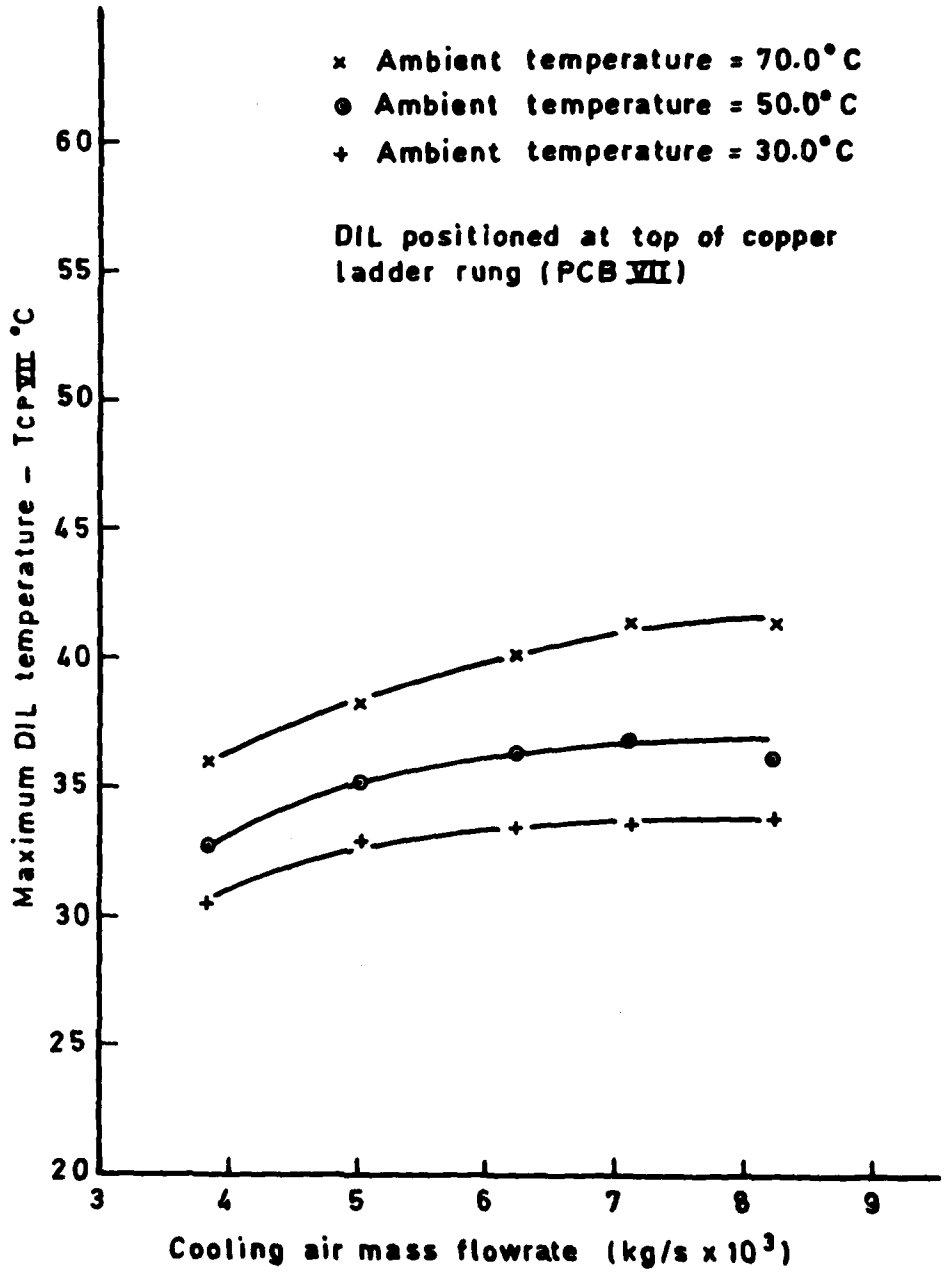

TR 82062

Fig 17 Variation of DIL temperature (relative to cold plate) with cooling air flow – DIL at top of rung

Fig 18

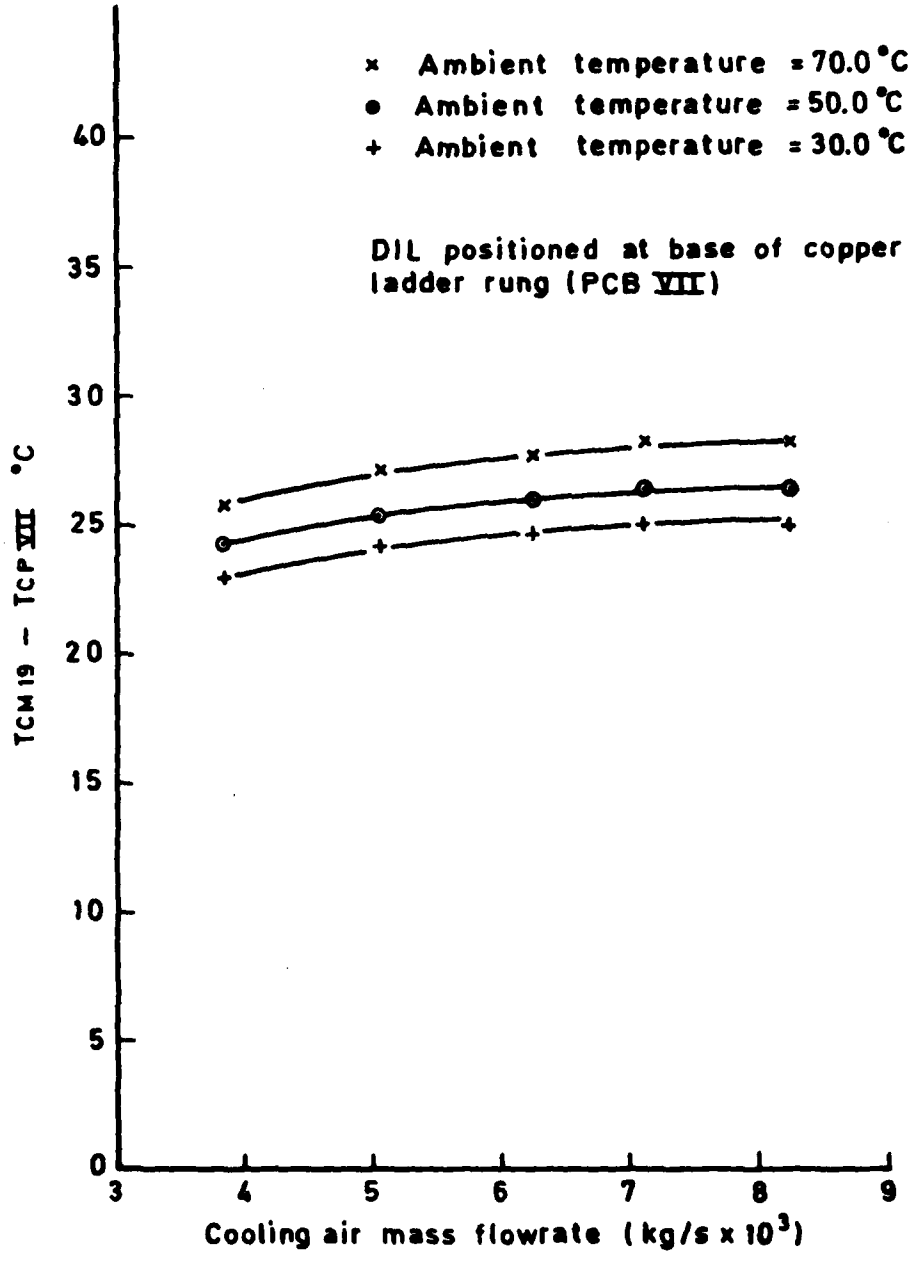

Fig 18 Variation of DIL temperature (relative to cold plate) with cooling air flow – DIL at base of rung

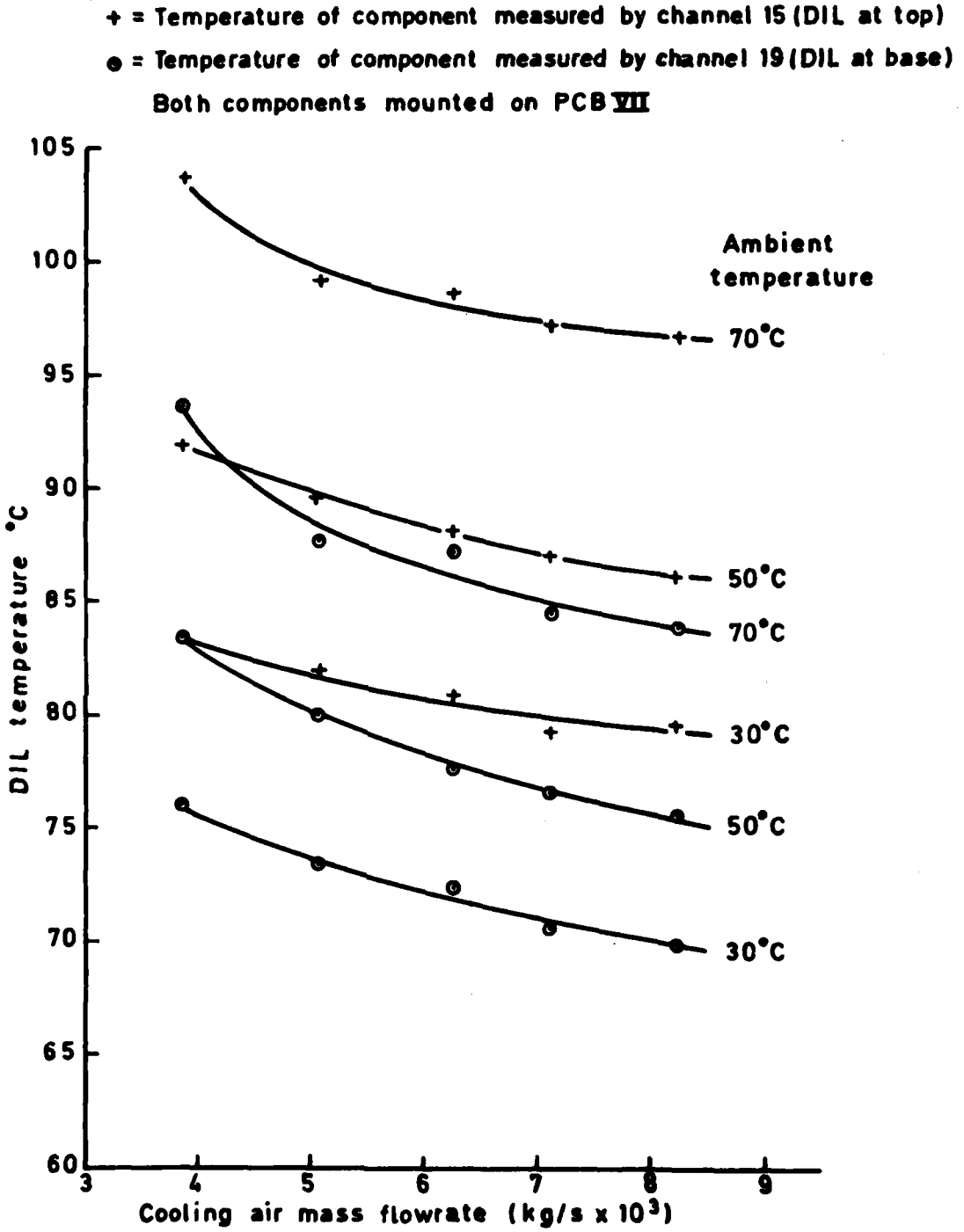

Fig 19 Variation of DIL temperatures (relative to cold plate) with cooling air flow – at two rung positions

Fig 20

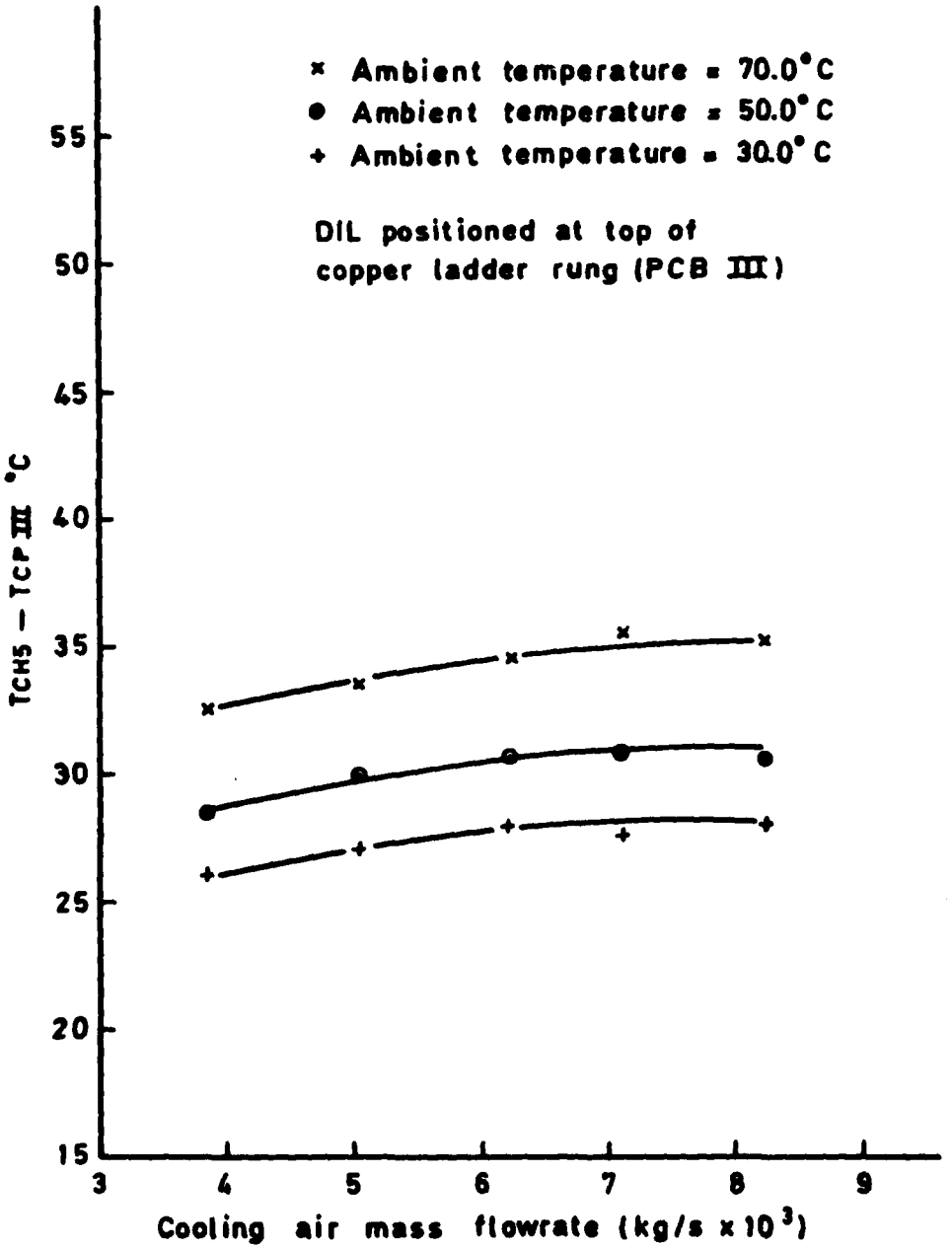

Fig 20 Variation of DIL temperature (relative to cold plate) with cooling air flow — DIL at top of rung

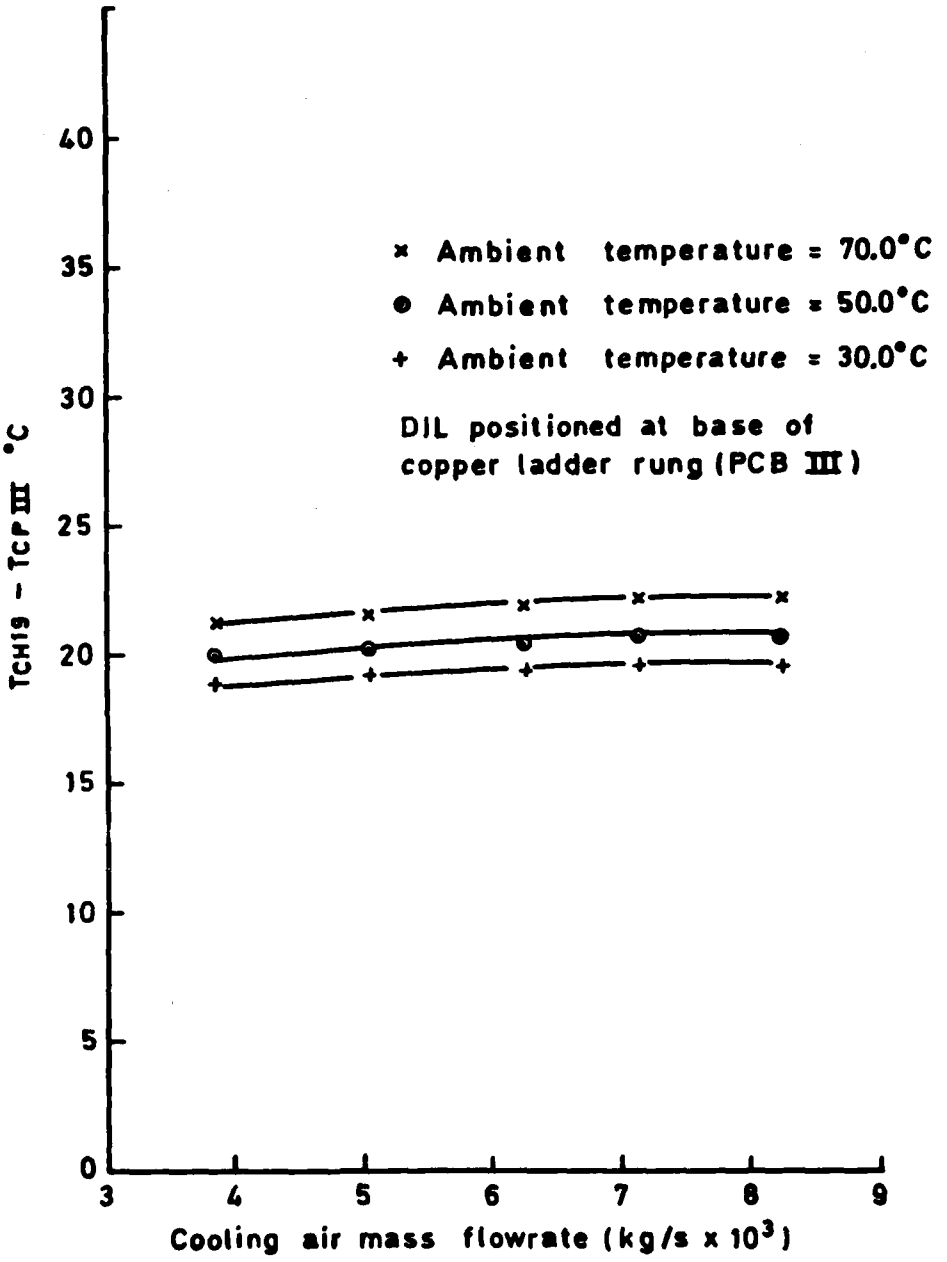

Fig 21 Variation of DIL temperature (relative to cold plate) with cooling air flow – DIL at base of rung

Fig 22

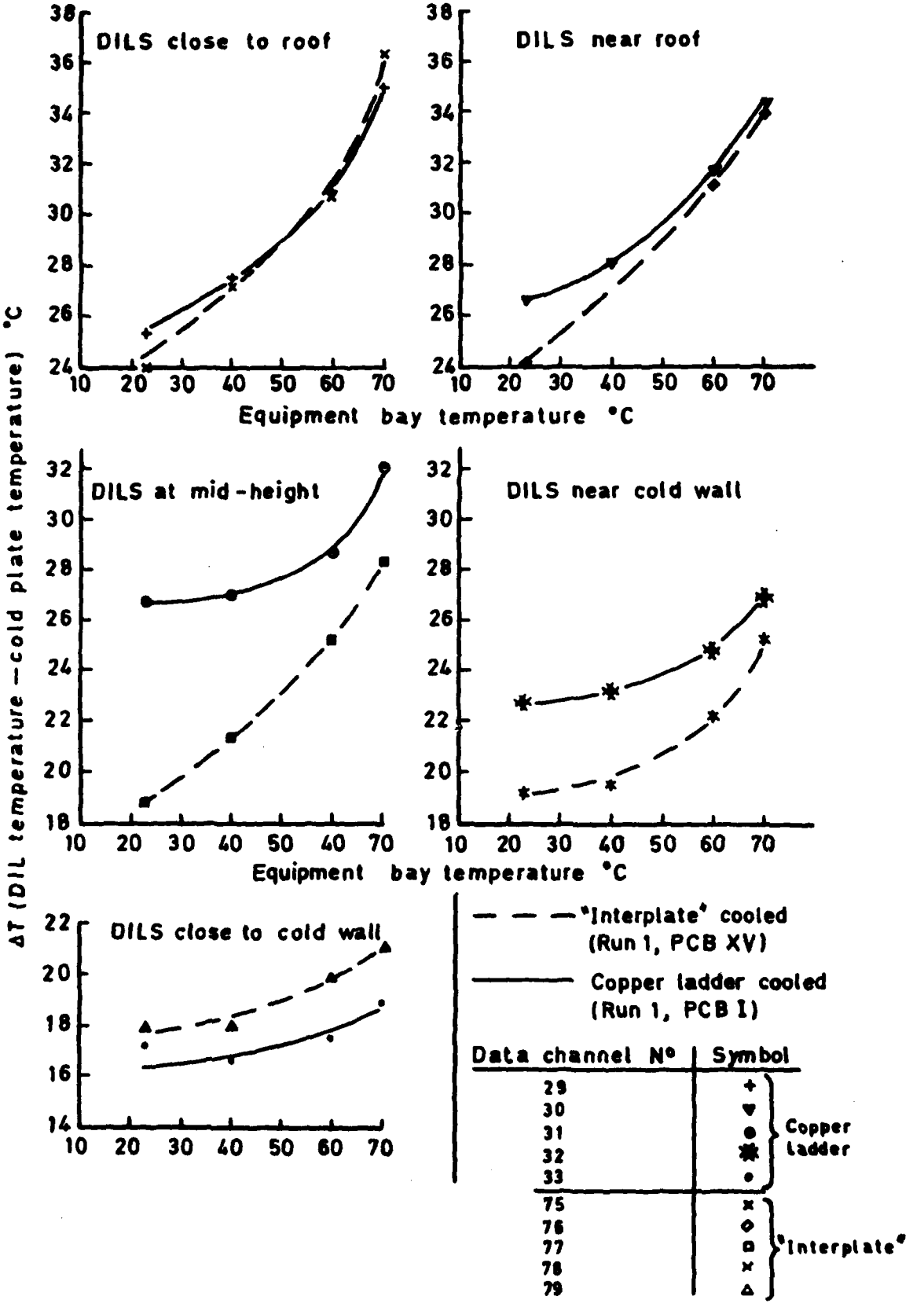

Fig 22 A comparison of copper ladder and interplate cooled DILs at various bay temperatures

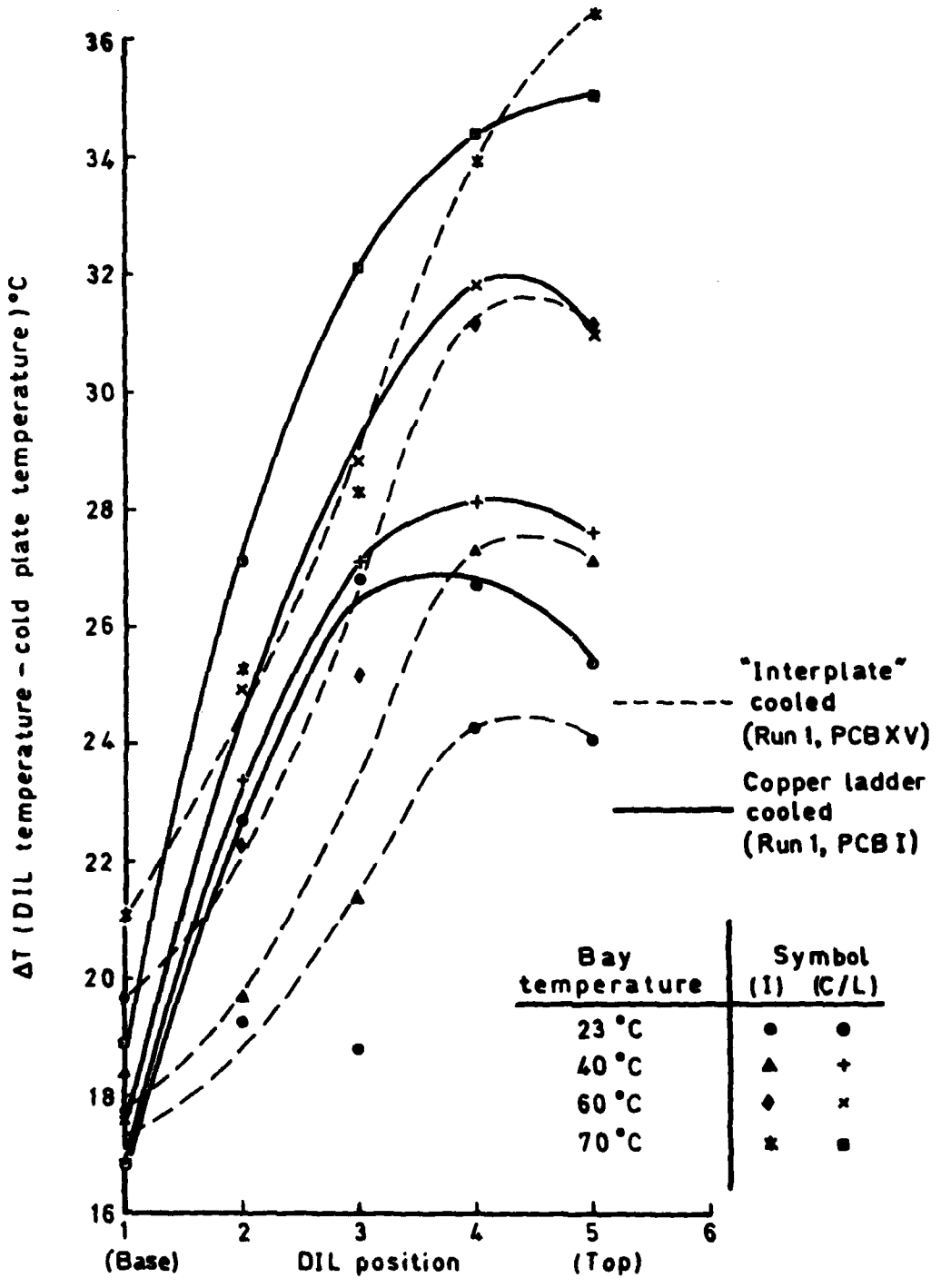

Fig 23 A comparison of copper ladder and interplate cooled DILs at various DIL positions